Title: Flattening of diurnal glucocorticoid oscillations causes Cd36 and insulin-mediated obesity

Authors: Stefan Tholen[1], Kyle M. Kovary[1], Atefeh Rabiee[1,2], Ewa Bielczyk-Maczyńska[1], Wenting Yang[1], Fredric B. Kraemer[3], and Mary N. Teruel[1,4,#]

Affiliations:
[1]Department of Chemical and Systems Biology, Stanford University, Stanford, CA, 94305, USA.
[2]Current address: Department of Physiology & Pharmacology, Thomas J. Long School of Pharmacy and Health Sciences, University of the Pacific, Stockton, CA 95211, USA.
[3]Dept. of Medicine/Division of Endocrinology, Stanford University, Stanford, CA and VA Palo Alto Health Care System, Palo Alto, CA 94305, USA.
[4]Department of Biochemistry and the Drukier Institute of Children's Health, Weill Cornell Medicine, NY, NY 10065, USA.
[#]**Corresponding Author and Lead Contact:** mnt4002@med.cornell.edu

Chronic stressors flatten diurnal glucocorticoid oscillations, resulting in obesity, insulin resistance, and diabetes. How such flattened diurnal glucocorticoid oscillations increase fat storage is unknown. Here we investigated the consequences in mice and found that flattening of glucocorticoid oscillations results not only in body weight gain, mainly due to increases in white fat depot mass, but also leads to hyperinsulinemia and fat accumulation in brown adipose tissue. A transcriptomic analysis of white and brown adipose tissues revealed that flattened glucocorticoid oscillations cause dysregulated lipid metabolism with a prominent role of the fatty acid transporter Cd36 and insulin-driven adipocyte hypertrophy. Indeed, *Cd36* knockout mice are partially protected against the adverse effects of flattened GC oscillations including body weight gain and lipid accumulation in the brown and visceral white fat depots. These results show the molecular mechanisms how flattened glucocorticoid oscillations can cause obesity and diabetes.

INTRODUCTION

Glucocorticoids are steroid hormones that are capable of causing tremendous shifts in carbohydrate and fatty acid metabolism throughout the body (Macfarlane et al., 2008). Glucocorticoids act on multiple tissues to increase available circulating energy substrates by promoting catabolism and deferring anabolism. A fundamental aspect of glucocorticoid regulation is that glucocorticoids are not maintained at constant levels in healthy mammals, but instead are secreted in diurnal oscillations (Weitzman et al., 1971) (Figure 1A, grey pattern). The diurnal pattern is essential for normal body function: the daily increase in glucocorticoids provides a wake-up signal and turns on whole body metabolism and the daily trough, or off-period, allows a rest period in which catabolic glucocorticoid-driven processes are not activated and the body can recover and reset (Dallman et al., 2000; Oster et al., 2017; Sapolsky et al., 1986).

The diurnal glucocorticoid pattern is controlled by the hypothalamic-pituitary-adrenal (HPA) axis which secretes glucocorticoids in response to light-dark signals from the master clock in the brain (Spiga et al., 2014). This same HPA axis also secretes glucocorticoids in response to stress. Short term, stress-mediated spikes in glucocorticoids are beneficial to increase overall catabolic activity and ready the body for a fight-or-flight response (Sapolsky et al., 1986). However, if the stress becomes chronic, the continual secretion of glucocorticoids flattens the normal diurnal oscillatory pattern, meaning that peak levels are decreased and trough levels are elevated, without the daily mean values significantly changing (Dallman et al., 2000) (Figure 1A, orange pattern). Such flattening of glucocorticoid oscillations can occur from depression, jet lag, aging, and irregular eating and sleeping schedules (Adam, 2017; Leproult et al., 1997), as well as in disease conditions such as Cushing's (Rossi et al., 2000), and has been shown to cause obesity and metabolic disease (Broussard and Van Cauter, 2016; Campbell et al., 2011; Dallman et al., 2000; Joseph and Golden, 2017; Mazziotti et al., 2011).

Fat mass expansion can occur both through adipogenesis, or the generation of new adipocytes from precursor cells, and from enlargement of existing adipocytes (hypertrophy)(Ghaben and Scherer,

2019). Previously we had studied the mechanisms controlling adipogenesis when glucocorticoids are flattened and found that the cause of the increased adipogenesis is that preadipocytes have a transcriptional network with slow and fast positive feedbacks centered on PPARG, the master regulator of adipogenesis, responses selectively to flattened, but not oscillating diurnal, glucocorticoid signals (Bahrami-Nejad et al., 2018). These results provided a molecular mechanism for the adipogenesis observed when glucocorticoid oscillations are flattened. However, the molecular mechanisms underlying the significant adipocyte hypertrophy when glucocorticoids are flattened remained poorly understood. Given the increasing evidence that the harmful metabolic effects of obesity originate primarily from adipocyte hypertrophy, rather than from adipogenesis (Ghaben and Scherer, 2019), it is of broad interest to determine the cause of the adipocyte hypertrophy when glucocorticoid oscillations are flattened.

That adipose tissue mass and adipocyte hypertrophy can increase when glucocorticoid oscillations are flattened (Bahrami-Nejad et al., 2018; Dallman et al., 2000; Karatsoreos et al., 2010; Rebuffé-Scrive et al., 1992; Shen et al., 2017) is puzzling since glucocorticoids are catabolic and generally drive breakdown of tissue mass. Indeed, other studies have shown that animals and humans can lose adipose tissue mass under some conditions when glucocorticoids are flattened (Lee et al., 2018; Peckett et al., 2011). We hypothesized that carrying out timecourse measurements would allow us to resolve these controversial results. In particular, we noted that the latter studies typically used high pharmacological doses of synthetic glucocorticoids or administered glucocorticoids together with a high fat diet which introduce confounding factors (Dunford and Riddell, 2016). Thus, to understand how obesity and adipocyte hypertrophy is generated just by glucocorticoid flattening, we used pellets containing corticosterone, the main physiological glucocorticoid in mice (Sapolsky et al., 1986), rather than synthetically stabilized types of glucocorticoids. We also avoided using high pharmacological doses and instead used experimental conditions that maintained normal mean circulating levels of glucocorticoids.

53 We designed timecourse experiments to mimic a limited period of chronic stress that flattens
54 glucocorticoid levels and we sought to answer three main questions: (i) how long does it take after
55 glucocorticoid flattening or glucocorticoid peak increases for adipocytes to become hypertrophic, (ii)
56 how long after glucocorticoid flattening do markers for metabolic disease in the plasma and liver start
57 to appear, and (iii) what is the mechanism that increases lipid storage in the hypertrophic adipocytes.
58 We found that within 3 days of glucocorticoid flattening, mice develop hyperinsulinemia and strongly
59 upregulate de novo fatty acid synthesis genes in white and brown adipose tissue as determined by
60 RNAseq. This latter result is surprising since lipid accumulation in adipocytes is thought to be
61 generated primarily from fatty acids taken up from the circulation (Santoro et al., 2021; Strawford et
62 al., 2004). Acute increases in brown adipose tissue mass and adipocyte hypertrophy were observed
63 starting at 3 days, followed by acute increases in white fat mass and adipocyte hypertrophy starting at
64 7 days. Despite a more than 2-fold increase in the brown and white fat mass size within 21 days, no
65 significant increase in circulating fatty acids or accumulation of lipid in the liver was observed,
66 supporting that the hyperinsulinemia and upregulation of de novo fatty acid synthesis in adipocytes
67 drive the hypertrophy. Experiments in mice in which the fatty acid transporter Cd36 was knocked out
68 support that increased fatty acid uptake also partially contributes to the adipocyte hypertrophy after
69 glucocorticoid flattening. Surprisingly, the hyperinsulinemia and much of the adipocyte hypertrophy
70 were reversed within 3 weeks after pellets stopped releasing glucocorticoid. Since the rapid increase
71 in adipocyte size results from uptake of both fatty acid and glucose from the circulation, the
72 hyperinsulinemia and adipocyte hypertrophy resulting from losing the glucocorticoid troughs likely
73 have initially a protective role to keep circulating fatty acids and glucose low. In this way, the rapid
74 increase in fat mass may serve to counteract the potentially harmful side effects of the catabolic activity
75 increase resulting from temporary stress and continuous glucocorticoids, as long as the stress
76 conditions do not exceed a few weeks.
77
78

RESULTS

Flattening of diurnal glucocorticoid oscillations causes rapid adipocyte hypertrophy in white and brown fat

To mimic the chronic stress condition, we flattened daily glucocorticoid oscillations in C57BL/6J male mice by implanting pellets that release corticosterone, the main glucocorticoid in mice, at a constant rate over 21 days. We specifically chose the dose of glucocorticoids that was released each day such that circulating glucocorticoid oscillations were flattened but the mean glucocorticoid level was kept approximately at normal physiological levels (Bahrami-Nejad et al., 2018; Hodes et al., 2012). As shown in Figure 1B, blood serum ELISA measurements confirmed that mice implanted with corticosterone pellets (hereafter referred to as “cort-pellet mice”) had decreased peak and increased trough levels of glucocorticoids compared to sham pellet-implanted mice (hereafter referred to as “sham-pellet mice”). Even though the mean glucocorticoid levels between the cort-pellet and sham-pellet mice were similar throughout the 21-day experiment, the mice with flattened glucocorticoid oscillations significantly increased their body weight compared to sham-pellet mice and ended up weighing 9.1% more (Figure 1C). As found in our previous study (Bahrami-Nejad et al., 2018) and in other studies which administered sustained glucocorticoids longterm (Bowles et al., 2015; Luijten et al., 2019), the increased weight gain in the cort-pellet mice cannot be explained by higher food intake (Figure 1d), and a reduction in metabolism may be a more significant contributing factor.

To assess whether the cort-pellet mice gain weight mainly by expansion of fat depots, we dissected and weighed the main white adipose tissue (WAT) and brown adipose tissue (BAT) depots in the mice. As the main subcutaneous WAT depot, we used the inguinal WAT which is a located in the flank region under the skin (Chusyd et al., 2016). As the main visceral WAT depot, we used the epididymal WAT which surrounds the gonads (Chusyd et al., 2016). We will hereafter refer to inguinal subcutaneous WAT as “sWAT”, and epididymal visceral WAT as “vWAT”. As the main brown fat depot, we used the interscapular brown fat depot which is the largest and most accessible brown fat depot in rodents (Cannon and Nedergaard, 2004). Strikingly, sWAT and vWAT weight increased more than

105 two-fold and BAT weight increased three-fold within 21 days of glucocorticoid oscillation flattening
106 (Figure 1E-1G, left two panels). Significant expansions of sWAT and vWAT were apparent after 7 days
107 of glucocorticoid flattening, and an even earlier expansion was observed in BAT after only 3 days
108 (Figure 1E-1G, left two panels). The expansions of WAT and BAT were confirmed by hematoxylin and
109 eosin (H&E) staining which revealed significantly increased cell volumes of the adipocytes in the BAT
110 from day 3 and in the WAT from day 7 (Figure 1E-1G, right two panels).

111 As a control to test whether the lipid accumulation in WAT and BAT shown in Figure 1 is due
112 to flattening of diurnal glucocorticoid oscillations and not caused by the amount of corticosterone
113 released into the mouse by the pellet, we injected C57BL/6J male mice at 5 PM each day for 21 days
114 with the same total amount of corticosterone that is released by the pellet in one day (Figure 2A). This
115 injection resulted in a more than 10-fold increase in the daily peak amplitude of corticosterone while
116 still maintaining the trough period (Figure 2B). Markedly, despite the higher peak level, corticosterone-
117 injected mice did not show a significant increase in body weight compared to sham-injected control
118 mice (Figure 2C). Furthermore, their food intake was not altered (Figure 2D). In addition, no differences
119 in fat pad weight were detected between the sWAT, vWAT, or BAT of the cort- and sham-injected
120 mice (Figure 2E-G), and histological analysis of the tissues showed no differences in lipid
121 accumulation (Figure S1).

122 Taken together, our results show that increasing the peak amplitude of corticosterone does
123 not affect body weight gain or lipid accumulation in the white fat depots. Thus, as previously shown
124 (Bahrami-Nejad et al., 2018), short spurts of glucocorticoids do not promote weight gain as long as
125 the increase in glucocorticoids occurs during the time window that glucocorticoids are normally high
126 and sufficiently long off-periods with low glucocorticoid levels are maintained. Furthermore, body
127 weight gain and lipid accumulation in WAT and BAT were only observed in the cort-pellet mice with
128 flattened glucocorticoids, despite the same total amount of glucocorticoid being introduced into both
129 cort-pellet and cort-injected mice, arguing that it is the glucocorticoid flattening and not the amount of
130 added glucocorticoids that is responsible for the adipocyte hypertrophy.

131

132 **Flattening of daily glucocorticoid oscillations does not result in fat deposition in the liver or**
133 **increased fatty acids or triglycerides in the circulation.**

134 Chronic or misregulated glucocorticoid secretion has been shown to increase fat mass in
135 rodents and humans, and the expansion of adipose tissue depots is accompanied by fat deposition in
136 the liver and an increase of triglycerides and fatty acids in blood plasma (Bowles et al., 2015; Campbell
137 et al., 2011; Chimin et al., 2014; Harris et al., 2013; Macfarlane et al., 2008). However, most *in vivo*
138 studies administrated high pharmacological doses of glucocorticoids or administered glucocorticoids
139 for several months which does not provide insight into how variations in normal physiological levels of
140 glucocorticoids of limited duration – such as are seen in chronic stress, jet lag, night shift work - affect
141 body metabolism. Since our experimental conditions use physiological levels of glucocorticoids and a
142 limited three-week period of glucocorticoid flattening, we tested to see if there is still fat accumulation
143 in liver. Markedly, histology analysis of the livers from cort-pellet mice showed no increase in lipid
144 accumulation or fat pad weight (Figure 3A), or upregulation of lipid metabolism genes in the liver
145 (Figure S2). Taken together, these results support that metabolic health is not yet strongly impacted
146 in other tissues other that fat even after 3 weeks of glucocorticoid flattening.

147 In another test of whether glucocorticoid flattening reduces overall metabolic health, we
148 checked for increases in circulating triglycerides, or glycerol and free fatty acids (FFA), which are the
149 building blocks of triglycerides. Given that triglycerides in adipose tissue are thought to be generated
150 primarily from fatty acids taken up from the circulation rather than from *de novo* synthesized fatty acids
151 (Santoro et al., 2021; Strawford et al., 2004), we expected to find that the adipocyte hypertrophy in
152 WAT and BAT was caused by higher fatty acid levels in the circulation. Surprisingly, we did not detect
153 significant differences in circulating glycerol, free fatty acids, or triglycerides between cort-pellet and
154 sham-pellet mice after 3 and 7 days of flattening glucocorticoid oscillations (Figure 3B). Furthermore,
155 what appeared as a small increase in these factors at day 14 was due primarily to reduced levels in
156 controls. Thus, increased fatty acid levels in the plasma are not responsible for the rapid initial phase

157 of adipocyte hypertrophy in observed in BAT and WAT during the first 2 weeks after glucocorticoid
158 flattening. These results suggest that the initial increase in adipocyte hypertrophy is not yet associated
159 with a loss of metabolic health. In control experiments, we confirmed that no significant lipid
160 accumulation in the liver (Figure 3C) or changes in triglyceride, glycerol, and free fatty acid levels
161 (Figure 3D) were detected when the same amount of corticosterone or control vehicle was injected
162 during the glucocorticoid peak period.
163
164 **The expansion of WAT and BAT is not due to defective thermogenesis**
165 Because we saw no lipid accumulation in the liver or significant lipid changes in the circulating
166 blood plasma, we concluded that the adipocyte hypertrophy must be originating from an adipose
167 tissue-intrinsic mechanism. It has been proposed that reduced thermogenesis due to defects in brown
168 fat function can indirectly contribute to white fat mass enlargement (Strack et al., 1995; VanDenBeukel
169 et al., 2014; Viengchareun et al., 2001). We thus focused next on asking whether a loss in brown fat
170 thermogenesis could indirectly explain the rapid lipid accumulation in WAT. We used RT-PCR (Figure
171 3E) and western blot analysis (Figure 3F) to monitor UCP1 mRNA and protein expression in BAT of
172 pellet-treated mice. Indeed, we did find reduced UCP1 in cort-pellet versus sham pellet mice, which is
173 expected to contribute to reduced thermogenesis. However, when the mice were placed at 4 degC in
174 an acute cold exposure experiment to compare their thermogenic capacities, we did not observe
175 significant differences in how core body temperatures dropped (Figure 3h), supporting that the
176 increased fat mass in the cort-pellet mice is not due to reduced thermogenesis despite reduced UCP1
177 expression in BAT (Luijten et al., 2019).
178 Taken together, the results so far suggest that adipocyte hypertrophy in response to
179 glucocorticoid flattening is not caused by changes in the liver, plasma lipid levels or thermogenesis,
180 suggesting that other metabolic changes in WAT and BAT are responsible. Since the primary role of
181 glucocorticoids is to regulate gene transcription, we next performed a transcriptome time-course

182 analysis of WAT and BAT tissues to understand whether transcription changes may cause the
183 development of acute adipocytes hypertrophy in response to glucocorticoid flattening.
184
185 **Flattening of glucocorticoid oscillations results in strong and rapid upregulation of de novo**
186 **fatty acid synthesis genes in WAT and BAT**
187 We set out to compare differences in the adipocyte transcriptomes between mice that had
188 oscillating versus flattened glucocorticoid levels. We focused on measuring gene expression in
189 visceral white adipose tissue (vWAT) since its expansion has been recognized to be detrimental to
190 metabolic health, while expansion of subcutaneous white adipose tissue (sWAT) may be protective
191 (Ghaben and Scherer, 2019). We also analyzed brown adipose tissue (BAT) because of increasing
192 evidence that BAT activity can significantly affect whole-body energy expenditure and fat tissue mass
193 (Cannon and Nedergaard, 2004; Saito, 2013). We implanted mice subcutaneously with corticosterone
194 or sham pellets and harvested vWAT and BAT between 1-5PM at four timepoints: 0, 3, 7, and 14
195 days after pellet implantation.
196 We carried out RNAseq analysis of vWAT and BAT in which we determined significant
197 differential gene expression by an FDR corrected p-value (qval) less than 0.05. Using this cutoff
198 criterion, we found several thousand transcripts were significantly changed in both vWAT and BAT
199 when glucocorticoid oscillations were flattened (cort-pellet versus sham-pellet mice) (Figure S3 and
200 Tables S4-S7). While the cort-pellet and sham-pellet samples were distinguishable from each other
201 using PCA analysis (Figure 4A and Figure S4A), the samples obtained at different timepoints (3, 7 or
202 14 days) in the two treatment groups were largely indistinguishable from each other, supporting that
203 flattening of glucocorticoid oscillations reprograms the vWAT and BAT transcriptomes within 3 days
204 and that the changes are sustained for at least 2 weeks thereafter. That significant changes in several
205 thousand genes of cort-pellet mice were already observed in vWAT at day 3 whereas expansion of
206 vWAT was only observed at day 7 (Figure 1F), suggests that the glucocorticoid-mediated changes in
207 the vWAT transcriptome help to drive the adipocyte hypertrophy in the vWAT, and not the other way

208 around. Because the gene expression changes at 3, 7, or 14 days were largely indistinguishable from
209 each other (Figure 4A), we combined the vWAT data from the three time points (3, 7, and 14 days) in
210 analysis of gene expression changes in vWAT after glucocorticoid flattening. Similarly, we found for
211 the BAT that gene expression changes at 3, 7, or 14 days in glucocorticoid flattened mice were largely
212 indistinguishable from each other (Figure S4A), and thus, we also combined the BAT data from the
213 three timepoints in our analysis of gene expression changes in BAT after glucocorticoid flattening.

214 In control experiments, we carried out RNAseq analysis of cort-injected and sham-injected
215 mice. As mentioned before, these mice were injected at 5PM each day with the same amount of
216 glucocorticoid released by the pellet per day. We sacrificed groups of mice between 1-5PM at four
217 timepoints: 0, 3, 7 or 14 days after the start of daily injections and collected and analyzed vWAT and
218 BAT by RNAseq. Remarkably, in comparing cort-injected versus sham-injected mice, PCA analysis
219 showed no significant differences between the two conditions (Figure 4B and Figure S4B).
220 Furthermore, no transcripts were changed in vWAT and only 9 transcripts were changed in BAT
221 between cort-injected and sham-injected mice compared to the thousands of significant transcript
222 changes observed in the vWAT and BAT between cort-pellet versus sham-pellet mice (Figure S3).
223 Thus, even a large increase in the peak amplitude of corticosterone does not manifest as a significant
224 change in gene expression in vWAT or BAT, consistent with our results in Figure 2 that showed no
225 increase in fat mass in the cort-injected or sham-injected mice. Interestingly, since the time between
226 injection of corticosterone at 5PM the day before until the mice were sacrificed between 1-5PM was
227 between 20-24 hours, the fact that there are no significant changes in gene expression in the vWAT
228 and BAT of cort-injected mice supports that the effect of glucocorticoids on gene expression is short-
229 lived – less than 24 hours - in adipose tissue.

230 As an additional control, to validate that daily injection and sham pellets do not cause stress
231 on their own that triggers gene expression changes, we compared sham-injected and sham pellet-
232 implanted mice. No differently expressed genes were observed when comparing vWAT or BAT of
233 these mice (Figure S3A-S3B), demonstrating that the procedure of pellet implantation and injections

234 themselves do not alter gene expression and supporting that the injection and pellet-mediated delivery
235 of glucocorticoid results can be directly compared.

236 Gene ontology (GO) analysis of the significantly regulated genes in vWAT of glucocorticoid
237 flattened mice identified “fatty acid biosynthetic process”, “acetyl-CoA metabolic process”, “pyruvate
238 metabolic process” and “glucose 6-phosphate metabolic process” as GO terms with high z-scores in
239 vWAT and BAT (Tables S2 and S3). In addition, GO terms were enriched that were related to lipid
240 uptake and utilization such as “lipid localization”, “fatty acid transport”, and “fatty acid metabolic
241 process”. Similar metabolic GO terms were also identified in BAT. This analysis suggested that
242 changes in adipocyte glucose and fatty acid metabolism may both contribute to the strong expansion
243 of the BAT and WAT mass.

244 To better understand how flattening of glucocorticoid oscillations could be changing glucose
245 and fatty acid metabolism in vWAT and BAT, we mapped our RNAseq data onto literature-curated
246 maps that position metabolic genes into the main pathways that contribute to the synthesis and
247 breakdown of triglycerides (Figure 4C and Figure S4). We colored each gene name by whether the
248 transcript is significantly increased (red), unchanged (black) or decreased (blue). A gene was
249 considered unchanged if the fold change was between 0.8 to 1.2 (less than 20% change). We used
250 bold type for the gene name if the increase or reduction is greater than 2-fold.

251 Due to the known catabolic role of glucocorticoid, we had initially expected that flattening
252 glucocorticoid oscillations would cause upregulation of the core lipolytic genes *Pnpla2* (*Atgl)*, *Lipe*
253 *(Hsl)*, and *Mgll.* However, these genes were either weakly or not upregulated in BAT or vWAT. In
254 contrast, we observed a striking upregulation of rate-limiting enzymes in the de novo fatty acid
255 synthesis pathway such as fatty acid synthase (*Fasn*), Acetyl-CoA carboxylase (*Acaca and Acacb*),
256 and *Acly*. We were surprised by this for two reasons. First, de novo fatty acid synthesis from glucose
257 is not generally believed to be a main contributor to triglyceride synthesis in vWAT. Rather the main
258 source of fatty acids to make triglycerides in adipocytes is thought to be fatty acids taken up from the
259 circulation (Santoro et al., 2021; Strawford et al., 2004). Second, expression of lipogenesis genes such

260 as Fasn and Acaca are known to be regulated by insulin signaling (Krycer et al., 2020; Song et al.,
261 2018). This raised the question whether the transcriptome changes and adipocyte hypertrophy in mice
262 with flattened glucocorticoid oscillations may at least in part be due to an increase in the level of insulin
263 in the blood plasma. Previous studies, for example, showed a link from insulin signaling to glucose
264 anabolism in adipocytes (Krycer et al., 2020).

265 Notably, there was a smaller upregulation of de novo fatty acid synthesis genes in BAT (Figure
266 S4C-S4D). Instead, BAT has a stronger upregulation of *Cd36* expression compared to vWAT and an
267 over 14-fold upregulation of *Gck* which is thought to be important in capturing glucose in cells
268 (Matschinsky and Wilson, 2019), suggesting that BAT may use a different strategy to increase fat
269 mass than vWAT when glucocorticoids are flattened and offering a possible explanation for the more
270 rapidly observed adipocyte hypertrophy in BAT versus WAT (Figure 1G),

271

272 **Glucocorticoid flattening results in rapidly induced hyperinsulinemia**

273 At the outset of our study, we did not consider that insulin might be elevated in the cort-pellet
274 since insulin is short-lived in the circulation and high or misregulated glucocorticoids levels are
275 commonly thought to inhibit insulin release from pancreatic beta cells (Delaunay et al., 1997).
276 However, we realized that hyperinsulinemia is common in human patients with flattened circulating
277 glucocorticoid levels such in subcritical hypercortisolism (Elhassan et al., 2019; Lopez et al., 2016;
278 Rossi et al., 2000). Furthermore, other studies have shown that hyperinsulinemia, even when glucose
279 was low, could originate from defects in insulin clearance (Bojsen-Møller et al., 2018; Protzek et al.,
280 2016)and also that glucocorticoid-stimulated pancreatic beta cells can in some cases still secrete
281 insulin (Fine et al., 2018). Taken together, it was plausible that high insulin could be responsible for
282 the gene expression profiles we had measured in mice with flattened glucocorticoid oscillations. We
283 thus carried out a timecourse analysis in which we monitored insulin levels in blood plasma over 21
284 days in the cort-pellet and sham-pellet mice.

285 Strikingly, we found that in mice with flattened corticosterone oscillations insulin levels
286 increased within 3 days to over 7 ng/ml compared to less than 1 ng/ml in sham pellet-implanted mice
287 (Figure 5A). This unexpectedly initial high insulin level then slowly decreased during the 21-days of
288 glucocorticoid flattening to about 3 ng/ml, which was still several fold higher than the insulin levels in
289 sham pellet-implanted mice. High insulin levels in mice and humans are typically correlated with high
290 glucose levels, such as occur after a meal, that stimulate pancreatic beta cells to secrete more insulin.
291 We were thus surprised to find that glucose levels are low in glucocorticoid-flattened mice, even slightly
292 lower than in control mice (Figure 5B). Since glucose levels are not high, this suggests that it is not
293 low glucose that signals to pancreatic beta cells to secrete more insulin. As alternative mechanisms,
294 glucocorticoids have been shown to reprogram pancreatic beta cells to cause continued insulin
295 secretion by increasing cAMP levels (Fine et al., 2018), as well as to cause decreased hepatic
296 clearance of insulin (Protzek et al., 2016).

297 Given the persistent high levels of insulin, we also considered that high insulin for continuous
298 periods of days and weeks may result in a loss of insulin sensitivity or ability to properly clear glucose
299 from the bloodstream. Thus, we carried out insulin and glucose tolerance tests (ITT and GTT) at
300 timepoints when insulin had been high for 17-21 days. Interestingly, as shown in the GTT test results
301 (Figure 5C), an intraperitoneally injected bolus of glucose was taken up even more rapidly in
302 glucocorticoid pellet-implanted mice compared to sham pellet control mice. The faster drop in glucose
303 seemed initially surprising but likely results from the higher level of insulin in the glucocorticoid pellet
304 implanted mice.

305 The fast clearance of a bolus of glucose in the GTT tests suggested that the glucocorticoid
306 flattened mice are still insulin sensitive. To test whether the mice are also still insulin sensitive despite
307 glucocorticoid-flattening and hyperinsulinemia, we carried out ITTs. We injected boluses of insulin into
308 the mice and measured whether glucose levels would drop within 30 minutes (Figure 5D). Indeed,
309 glucose levels in glucocorticoid flattened mice dropped similarly as in the control mice, albeit slightly
310 slower, supporting that corticosterone pellet-implanted mice are still insulin sensitive but have a weak

311 form of insulin-resistance. The hyperinsulinemia when glucocorticoid oscillations are flattened,
312 together with the maintenance of insulin sensitivity, can explain the observed slightly lower-than-
313 normal glucose levels since insulin promotes glucose uptake into fat and muscle [43]. Interestingly, the
314 lower blood glucose levels (Figure 5B), and thus likely lower metabolism in the glucocorticoid-flattened
315 mice, provides an explanation for why these mice are able to gain weight, even though we found no
316 change in food intake during 3 weeks of glucocorticoid flattening (Figure 1D).

317 In control experiments, mice injected with the same dose of glucocorticoid as released by the
318 pellet per day did not reveal any differences in glucose tolerance compared to sham injected mice and
319 did not display higher insulin levels in the blood plasma (Figures 5E-5F). Together, these results show
320 that flattening of glucocorticoids causes hyperinsulinemia that occurs within 3 days, before adipocyte
321 hypertrophy is observed in WAT.

322

323 **Metabolic changes caused by 3 weeks of flattening glucocorticoids are largely reversible**

324 One of the goals of this study was to mimic a temporary three week-long stress condition and
325 accordingly chose a pellet that releases corticosterone over 3 weeks. During the three weeks of
326 glucocorticoid flattening, we observed hyperinsulinemia and significant adipocyte hypertrophy which
327 are typically considered to be harmful for metabolic health. It was therefore surprising that mice were
328 able to maintain low glucose levels and insulin sensitivity, which are markers of a healthy metabolic
329 state, for the three weeks in which glucocorticoid were flattened. Furthermore, the levels of fatty acids
330 and triglyceride in the circulation were only minimally increased and no lipid accumulation was
331 observed in the liver (Figure 3), further suggesting that mice in which glucocorticoids are flattened
332 even for up to 3 weeks are still metabolically healthy, despite significant weight gain, adipose tissue
333 hypertrophy, and hyperinsulinemia.

334 Strikingly, the hyperinsulinemia in glucocorticoid flattened mice was fully reversible. Insulin
335 levels returned to the levels of the sham-pellet mice at 42 days, which is 3 weeks after the time when
336 the implanted pellet stops releasing corticosterone (Figure 6A). These results support a direct role for

337 flattening of glucocorticoid oscillations in driving the hyperinsulinemia. Furthermore, about half of the
338 weight gain in WAT and all the weight gain in BAT were lost at 42 days (Figure 6B). There was
339 variability between mice, and many restored their fat mass to that of control mice at that time. Together,
340 these results suggest that the greater than two-fold increase in adipocyte hypertrophy is mostly
341 reversible in WAT and fully reversible in BAT over a similar time period as it took to increase the fat
342 mass. However, it should be noted that while the healthy low trough glucocorticoid levels were restored
343 by 3 weeks after the pellet stopped releasing glucocorticoid (Figure S5), the peak levels during waking
344 remained reduced in most of the mice, suggesting that the 3-week glucocorticoid flattening has a
345 longer-term impact on the diurnal control of glucocorticoid secretion from the adrenal cortex.

346 We conclude that glucocorticoid flattening rapidly induces white and brown adipocyte
347 hypertrophy, causing WAT and BAT to more than double in only three weeks, but the increase in fat
348 mass remains mostly reversible and the hyperinsulinemia remains fully reversible. These results
349 support that there is a healthy "alert" state of intermediate duration that mice can assume for weeks in
350 response to temporary stress and continually activated glucocorticoid signaling. This alert state has a
351 protective role by keeping the levels of fatty acid and glucose in the circulation in check due to high
352 circulating insulin and high glucose uptake rates. The existence of this alert state is intriguing since
353 most previous work has described stress as being either acute, fight-or-flight response glucocorticoid
354 increases or chronic long-term stress that would cause irreversible adipocyte dysfunction and
355 associated metabolic diseases (McEwen, 2000; Sapolsky, 2004; Sapolsky et al., 1986). Before this
356 study, our assumption had been that adipocyte hypertrophy caused by a chronic three-week long
357 glucocorticoid flattening would be irreversible. However, our data shows that this alert state is
358 reversible, and mice can recover from the hyperinsulinemia and adipocyte hypertrophy, as long as the
359 stress and glucocorticoid flattening does not exceed a few weeks. Taken together, these results
360 suggest that there should be a modification to the commonly discussed distinction between an acute,
361 fight-or-flight type glucocorticoid response on the order of hours, and a chronic permanent
362 glucocorticoid dysregulation (McEwen, 2000; Sapolsky, 2004; Sapolsky et al., 1987). Our study

363 suggests that one should add a reversible alert state of intermediate duration, approximately of 3
364 weeks. Based on previous studies that used longer glucocorticoid flattening (Dunford and Riddell,
365 2016; Lee et al., 2018), this intermediate state would then transition to a chronic irreversible state if
366 the stress lasts much longer or glucocorticoid signals are elevated (Figure 6C, yellow box).
367

368 **CD36ko mice are partially protected against weight gain induced by flattening of glucocorticoid**
369 **oscillations**

370 The hyperinsulinemia (Figure 5) and large metabolic transcriptome changes in WAT and BAT
371 (Figure 4) are already fully induced within three days of flattening of glucocorticoid oscillations, which
372 is before expansion of WAT depots is observed. Since insulin is known to mediate many of the
373 transcriptome changes observed after 3 days, a likely order of events is that mice with flattened
374 glucocorticoid rapidly develop hyperinsulinemia which then causes insulin-driven upregulation of fatty
375 acid synthesis genes such as *Fasn, Acaca,* and *Gck* in fat cells. Upregulation of these genes would
376 increase conversion of glucose into fatty acids and increase triglyceride synthesis, explaining the
377 adipocyte hypertrophy observed a few days later.

378 We nevertheless considered that the adipocyte hypertrophy could also be partially due to
379 increased fatty acid uptake, especially since Cd36, a high-affinity receptor for long-chain fatty acids
380 that facilitates fatty acid uptake into muscle and adipose tissues of rodents and humans(Pepino et al.,
381 2014), has been shown to be glucocorticoid-regulated (Yu et al., 2010). Our RNAseq analysis had
382 shown that CD36 gene expression levels are upregulated in both vWAT and BAT of cort-pellet mice
383 (Figures 4C, 4D, S4C, and S4D). RT-PCR analysis confirmed that Cd36 was indeed upregulated
384 (Figure 7A), We thus went forward with investigating CD36's role in adipocyte hypertrophy when
385 glucocorticoid oscillations are flattened.

386 We implanted Cd36ko and wildtype mice with corticosterone or sham pellets for 21 days and
387 then dissected and weighed their sWAT, vWAT and BAT tissues. As had been observed previously in
388 Figures 1E-1G, flattening glucocorticoid oscillations in wildtype mice increased vWAT, sWAT and BAT

389 weight more than two-fold over control mice (dark blue compared to red; Figure 7B). Remarkably,
390 knocking out Cd36 resulted in a much smaller increase in weight for all three fat tissue types (light
391 blue compared to orange; Figure 7B). Histological analysis of the three fat tissue types showed that
392 adipocytes of cort-pellet Cd36ko mice displayed lower increases in cell volume than cort-pellet
393 wildtype mice (Figure 7C; quantification is shown in Figure S6), further supporting that at least part of
394 the adipose hypertrophy in glucocorticoid flattened mice is caused by Cd36-mediated fatty acid uptake.
395 Although loss of Cd36 significantly reduces the adipocyte hypertrophy in WAT and BAT upon
396 flattening corticosterone oscillations, the cort-pellet Cd36ko mice still have hyperinsulinemia (Figure
397 7D) and lower blood glucose levels (Figure 7E), similar to the cort-pellet wildtype mice. That the rescue
398 of adipocyte hypertrophy in Cd36ko mice is only partial is consistent with the interpretation that the
399 remaining hypertrophy is the result of hyperinsulinemia. Together, these results suggest that adipocyte
400 hypertrophy in response to glucocorticoid flattening is caused by a combination of Cd36-mediated
401 uptake of fatty acids and hyperinsulinemia-mediated increases in glucose uptake and de novo fatty
402 acid synthesis from glucose.

403 **DISCUSSION**

404 Flattening of daily glucocorticoid oscillations in rodents and humans due to Cushing's disease
405 and chronic stress has been shown to cause obesity and metabolic disease (Bahrami-Nejad et al.,
406 2018; Campbell et al., 2011; Chimin et al., 2014; Dallman et al., 2000; Joseph and Golden, 2017;
407 Karatsoreos et al., 2010; Rossi et al., 2000), with adipocyte hypertrophy believed to be a main
408 contributing factor. Here we sought to understand the mechanisms underlying the adipocyte
409 hypertrophy by varying the timing of how glucocorticoids were applied to mice and measuring relevant
410 parameters in blood and tissues at multiple timepoints. Strikingly, within 3 days, circulating insulin
411 levels became persistently high and thousands of transcripts in WAT and BAT changed. These effects
412 preceded the adipocyte hypertrophy and expansion of WAT observed at 7 days in the white fat (WAT).

413 Since adipocyte hypertrophy is typically associated with increased fatty acids and triglycerides
414 in the circulation and increased fat deposition in the liver (Campbell et al., 2011; Harris et al., 2013),
415 we were surprised to find no increase in circulating fatty acid levels and no measurable fat deposition
416 in the liver. Furthermore, because hyperinsulinemia is typically closely associated with high glucose
417 levels, we were also surprised to find that circulating glucose levels were even slightly lower in mice
418 with flattened glucocorticoids and hyperinsulinemia, compared to control animals. An explanation for
419 the low glucose levels is that even after 3 weeks of glucocorticoid flattening and significant
420 hyperinsulinemia and adipocyte hypertrophy, the mice are still able to uptake glucose into peripheral
421 tissues at even a higher rate compared to control mice, as demonstrated by a glucose tolerance test.
422 These results suggests that the significant adipocyte hypertrophy observed in the glucocorticoid
423 flattened mice is initially not causing a loss of metabolic health.
424 It has generally been assumed that most of the lipid stored in adipocytes is synthesized from
425 fatty acids taken up from the circulation, rather than being synthesized from glucose (Digirolamo et al.,
426 1992; Santoro et al., 2021). However, our analysis of CD36 knockout mouse showed that increased
427 fatty acid uptake was only partially responsible for the adipocyte hypertrophy. For conditions in which
428 insulin is high and glucose is low, as we observe in glucocorticoid flattened mice, glucose uptake is
429 accelerated, and the significant upregulation of de novo fatty acid synthesis genes observed in vWAT
430 and BAT in our RNAseq analysis support that the percentage of glucose converted to triglycerides is
431 high. Furthermore, the lack of increase in lipolytic genes in vWAT and BAT and low circulating free
432 fatty acids support that the newly synthesized triglycerides are retained in the adipocytes. Taken
433 together, our results argue that increased insulin-mediated glucose uptake, de novo synthesis of fatty
434 acids from glucose, and suppression of lipolysis in adipocytes drive the adipocyte hypertrophy in the
435 glucocorticoid-flattened mice. The hyperinsulinemia we observed when glucocorticoids are flattened
436 is consistent with observations in human patient studies of subcritical hypercortolism (Papanastasiou
437 et al., 2017; Rossi et al., 2000). Further studies are needed to determine the cause of the
438 hyperinsulinemia in the absence of increased glucose when glucocorticoids are flattened and whether

439 it be due to increased insulin secretion from pancreatic beta cells or reduced insulin clearance in the
440 liver requires further study (Bojsen-Møller et al., 2018; Protzek et al., 2016).

441 The implanted pellet was designed to release corticosterone at a constant rate for 21 days.
442 Interestingly, analysis of mice at 42 days, three weeks after the glucocorticoid flattening stimulus
443 ceased, showed that the hyperinsulinemia was completely reversed, glucocorticoid levels during the
444 trough period had returned to basal levels, and about half of the gain in WAT mass and all of the gain
445 in BAT mass were reversed as well. We further found normal levels of circulating FFAs and no lipid
446 accumulation in the liver after 2-3 weeks of glucocorticoid flattening, supporting that there is no
447 significant loss of metabolic health during this period, despite a more than doubling of fat mass and
448 lipid accumulation in WAT and BAT. Nevertheless, there were signs for longer term effects on the
449 overall metabolism in mice after 3 weeks of glucocorticoid flattening. Even after the CORT pellet had
450 ceased to release corticosterone for 3 weeks, white fat mass in both vWAT and sWAT were still 50%
451 higher and the normally high peak levels of corticosterone during waking were not yet fully restored.
452 There was much variability between mice with some returning to normal fat mass levels but others
453 keeping a higher mass. Nevertheless, taken together, despite the more than doubling of fat mass, our
454 studies suggest that cells remain metabolically healthy up to a 3-week period of glucocorticoid
455 flattening before flattening of glucocorticoids ends up causing metabolic disease and diabetes..

456 A plausible overall interpretation of our results is that glucocorticoid flattening leads to a
457 metabolic “alert” state that is distinct from the initial rapid fight-or-flight response and distinct from the
458 chronic stress state that is associated with metabolic diseases. This alert state is marked by
459 persistently high insulin and increased Cd36-mediated fatty acid uptake into adipocytes that results in
460 normal glucose and fatty acid levels in the circulation (Figure 7F). For periods of up to three weeks, a
461 gradual increase in adipose hypertrophy helps maintain the alert state by accelerated uptake of
462 glucose and fatty acid. The cost of maintaining this alert state for three weeks is a greater than two-
463 fold increase in white and brown adipose mass due to continued uptake of fatty acids and glucose into
464 WAT and BAT that ultimately results in metabolic disease.

465 In summary, our study shows the cellular and physiological consequences of temporary
466 flattening of glucocorticoids that is frequently observed during chronic stress. We show that loss of the
467 normal diurnal glucocorticoid oscillation pattern can result in acute hyperinsulinemia and acute
468 hypertrophy in which white and brown fat mass more than doubles within 3 weeks. The rapid increase
469 in white and brown fat mass is mediated by a combination of insulin-mediated upregulation of glucose
470 conversion to fatty acid and Cd36-mediated fatty acid uptake. Remarkably, for up to about 3 weeks,
471 fatty acids and glucose levels in the circulation remain near normal levels and much of the metabolic
472 changes associated with poor metabolic health remain reversible. Furthermore, much of the gain in
473 white fat mass and all of the gain in brown fat mass can be reversed when glucocorticoid flattening
474 stops. Continued fatty acid and glucose uptake into fat tissue can therefore minimize the damage that
475 could be caused by hyperglycemia and high lipid levels in the circulation resulting from glucocorticoid-
476 mediated catabolism. Thus, to maintain the alert status for a potential fight-or-flight response, the
477 hyperinsulinemia and adipocyte hypertrophy induced by glucocorticoid flattening are unexpectedly
478 protective for metabolic health for a period of a few weeks.
479

480 **REFERENCES**

481 Adam, E.K. (2017). Diurnal Cortisol Slopes and Mental and Physical Health Outcomes:A Systematic
482 Review and Meta-analysis. Psychoneuroendcrinology *Sep*, 25–41.

483 Bahrami-Nejad, Z., Zhao, M.L., Tholen, S., Hunerdosse, D., Tkach, K.E., van Schie, S., Chung, M.,
484 and Teruel, M.N. (2018). A Transcriptional Circuit Filters Oscillating Circadian Hormonal Inputs to
485 Regulate Fat Cell Differentiation. Cell Metab. *27*, 854-868.e8.

486 Bojsen-Møller, K.N., Lundsgaard, A.M., Madsbad, S., Kiens, B., and Holst, J.J. (2018). Hepatic
487 insulin clearance in regulation of systemic insulin concentrations-role of carbohydrate and energy
488 availability. Diabetes *67*, 2129–2136.

489 Bowles, N.P., Karatsoreos, I.N., Li, X., Vemuri, V.K., Wood, J.-A., Li, Z., Tamashiro, K.L.K.,
490 Schwartz, G.J., Makriyannis, A.M., Kunos, G., et al. (2015). A peripheral endocannabinoid
491 mechanism contributes to glucocorticoid-mediated metabolic syndrome. Proc. Natl. Acad. Sci. *112*,
492 285–290.

493 Broussard, J.L., and Van Cauter, E. (2016). Disturbances of sleep and circadian rhythms: Novel risk
494 factors for obesity. Curr. Opin. Endocrinol. Diabetes Obes. *23*, 353–359.

495 Campbell, J.E., Peckett, A.J., D'Souza, A.M., Hawke, T.J., and Riddell, M.C. (2011). Adipogenic and
496 lipolytic effects of chronic glucocorticoid exposure. Am. J. Physiol. - Cell Physiol. *300*, C198-209.

497 Cannon, B., and Nedergaard, J. (2004). Brown Adipose Tissue: Function and Physiological
498 Significance. Physiol. Rev. *84*, 277–359.

499 Chimin, P., Farias, T.D.S.M., Torres-Leal, F.L., Bolsoni-Lopes, A., Campaña, A.B., Andreotti, S., and
500 Lima, F.B. (2014). Chronic glucocorticoid treatment enhances lipogenic activity in visceral
501 adipocytes of male Wistar rats. Acta Physiol. *211*, 409–420.

502 Chusyd, D.E., Wang, D., Huffman, D.M., and Nagy, T.R. (2016). Relationships between Rodent
503 White Adipose Fat Pads and Human White Adipose Fat Depots. Front. Nutr. *3*.

504 Dallman, M.F., Akana, S.F., Bhatnagar, S., Bell, M.E., and Strack, A.M. (2000). Bottomed out:
505 Metabolic significance of the circadian trough in glucocorticoid concentrations. Int. J. Obes. *24*, S40–
506 S46.

507 Delaunay, F., Khan, A., Cintra, A., Davani, B., Ling, Z.C., Andersson, A., Östenson, C.G.,
508 Gustafsson, J.Å., Efendic, S., and Okret, S. (1997). Pancreatic β cells are important targets for the
509 diabetogenic effects of glucocorticoids. J. Clin. Invest. *100*, 2094–2098.

510 Digirolamo, M., Newby, F.D., and Lovejoy, J. (1992). Lactate production in adipose tissue; a
511 regulated function with extra-adipose implications. FASEB J. *6*, 2405–2412.

512 Dunford, E.C., and Riddell, M.C. (2016). The Metabolic Implications of Glucocorticoids in a High-Fat
513 Diet Setting and the Counter-Effects of Exercise.

514 Elhassan, Y.S., Alahdab, F., Prete, A., Delivanis, D.A., Khanna, A., Prokop, L., Murad, M.H.,
515 O'Reilly, M.W., Arlt, W., and Bancos, I. (2019). Natural History of Adrenal Incidentalomas with and
516 without Mild Autonomous Cortisol Excess A Systematic Review and Meta-analysis. Ann. Intern.
517 Med. *171*, 107–116.

518 Febbraio, M., Abumrad, N.A., Hajjar, D.P., Sharma, K., Cheng, W., Pearce, S.F.A., and Silverstein,
519 R.L. (1999). A null mutation in murine CD36 reveals an important role in fatty acid and lipoprotein
520 metabolism. J. Biol. Chem. *274*, 19055–19062.

521 Fine, N.H.F., Doig, C.L., Elhassan, Y.S., Vierra, N.C., Marchetti, P., Bugliani, M., Nano, R., Piemonti,
522 L., Rutter, G.A., Jacobson, D.A., et al. (2018). Glucocorticoids reprogram b-cell signaling to preserve
523 insulin secretion. Diabetes *67*, 278–290.

524 Galarraga, M., Campión, J., Muñoz-Barrutia, A., Boqué, N., Moreno, H., Martínez, J.A., Milagro, F.,
525 and Ortiz-de-Solórzano, C. (2012). Adiposoft: automated software for the analysis of white adipose
526 tissue cellularity in histological sections. J. Lipid Res. *53*, 2791–2796.

527 Ghaben, A.L., and Scherer, P.E. (2019). Adipogenesis and metabolic health. Nat. Rev. Mol. Cell
528 Biol. *20*, 242–258.

529 Harris, C., Roohk, D.J., Fitch, M., Boudignon, B.M., Halloran, B.P., and Hellerstein, M.K. (2013).
530 Large increases in adipose triacylglycerol flux in cushingoid CRH-Tg mice are explained by futile
531 cycling. Am. J. Physiol. - Endocrinol. Metab. *304*, 282–293.

532 Hodes, G.E., Brookshire, B.R., Hill-Smith, T.E., Teegarden, S.L., Berton, O., and Lucki, I. (2012).
533 Strain differences in the effects of chronic corticosterone exposure in the hippocampus.
534 Neuroscience *222*, 269–280.

535 Joseph, J.J., and Golden, S.H. (2017). Cortisol dysregulation : the bidirectional link between stress ,
536 depression , and type 2 diabetes mellitus. *1391*, 20–34.

537 Karatsoreos, I.N., Bhagat, S.M., Bowles, N.P., Weil, Z.M., Pfaff, D.W., and McEwen, B.S. (2010).
538 Endocrine and physiological changes in response to chronic corticosterone: A potential model of the
539 metabolic syndrome in mouse. Endocrinology *151*, 2117–2127.

540 Krycer, J.R., Quek, L.E., Francis, D., Zadoorian, A., Weiss, F.C., Cooke, K.C., Nelson, M.E., Diaz-
541 Vegas, A., Humphrey, S.J., Scalzo, R., et al. (2020). Insulin signaling requires glucose to promote
542 lipid anabolism in adipocytes. J. Biol. Chem. *295*, 13250–13266.

543 Lee, R.A., Harris, C.A., and Wang, J.-C. (2018). Glucocorticoid Receptor and Adipocyte Biology.
544 Nucl. Recept. Res. *5*, 1–21.

545 Leproult, R., Copinschi, G., Buxton, O., and Van Cauter, E. (1997). Sleep loss results in an elevation
546 of cortisol levels the next evening. Sleep *20*, 865–870.

547 Lopez, D., Luque-Fernandez, M.A., Steele, A., Adler, G.K., Turchin, A., and Vaidya, A. (2016).
548 "Nonfunctional" adrenal Tumors and the risk for incident diabetes and cardiovascular outcomes: A
549 cohort study. Ann. Intern. Med. *165*, 533–542.

550 Luijten, I.H.N., Brooks, K., Boulet, N., Shabalina, I.G., Jaiprakash, A., Carlsson, B., Fischer, A.W.,
551 Cannon, B., and Nedergaard, J. (2019). Glucocorticoid-Induced Obesity Develops Independently of
552 UCP1. Cell Rep. *27*, 1686-1698.e5.

553 Macfarlane, D.P., Forbes, S., and Walker, B.R. (2008). Glucocorticoids and fatty acid metabolism in
554 humans: Fuelling fat redistribution in the metabolic syndrome. J. Endocrinol. *197*, 189–204.

555 Matschinsky, F.M., and Wilson, D.F. (2019). The central role of glucokinase in glucose homeostasis:
556 A perspective 50 years after demonstrating the presence of the enzyme in islets of Langerhans.
557 Front. Physiol. *10*.

558 Mazziotti, G., Gazzaruso, C., and Giustina, A. (2011). Diabetes in Cushing syndrome : basic and
559 clinical aspects. Trends Endocrinol. Metab. *22*, 499–506.

560 McEwen, B.S. (2000). Allostasis and allostatic load: Implications for neuropsychopharmacology.
561 NEUROPSYCHOPHARMACOLOGY *22*, 108–124.

562 Oster, H., Challet, E., Ott, V., Arvat, E., de Kloet, E.R., Dijk, D.J., Lightman, S., Vgontzas, A., and
563 Van Cauter, E. (2017). The functional and clinical significance of the 24-hour rhythm of circulating
564 glucocorticoids. Endocr. Rev. *38*, 3–45.

565 Papanastasiou, L., Alexandraki, K., Androulakis, I.I., Fountoulakis, S., Kounadi, T., Markou, A.,
566 Tsiavos, V., Samara, C., Papaioannou, T.G., Piaditis, G., et al. (2017). Concomitant alterations of
567 metabolic parameters, cardiovascular risk factors and altered cortisol secretion in patients with
568 adrenal incidentalomas during prolonged follow-up. Clin. Endocrinol. (Oxf). *86*, 488–498.

569 Peckett, A.J., Wright, D.C., and Riddell, M.C. (2011). The effects of glucocorticoids on adipose
570 tissue lipid metabolism. Metabolism. *60*, 1500–1510.

571 Pepino, M.Y., Kuda, O., Samovski, D., and Abumrad, N.A. (2014). Structure-Function of CD36 and
572 Importance of Fatty Acid Signal Transduction in Fat Metabolism. Annu. Rev. Nutr. *34*, 281–303.

573 Protzek, A.O.P., Rezende, L.F., Costa-Júnior, J.M., Ferreira, S.M., Cappelli, A.P.G., Paula, F.M.M.
574 De, Souza, J.C. De, Kurauti, M.A., Carneiro, E.M., Rafacho, A., et al. (2016). Hyperinsulinemia
575 caused by dexamethasone treatment is associated with reduced insulin clearance and lower hepatic
576 activity of insulin-degrading enzyme. J. Steroid Biochem. Mol. Biol. *155*, 1–8.

577 Rebuffé-Scrive, M., Walsh, U.A., McEwen, B., Rodin, J., Rebuffe-Scrive, M., Walsh, U.A., McEwen,
578 B., and Rodin, J. (1992). Effect of chronic stress and exogenous glucocorticoids on regional fat
579 distribution and metabolism. Physiol. Behav. *52*, 583–590.

580 Rossi, R., Tauchmanova, L., Luciano, A., Di Martino, M., Battista, C., Del Viscovo, L., Nuzzo, V., and
581 Lombardi, G. (2000). Subclinical Cushing's syndrome in patients with adrenal incidentaloma: Clinical
582 and biochemical features. J. Clin. Endocrinol. Metab. *85*, 1440–1448.

583 Saito, M. (2013). Brown adipose tissue as a regulator of energy expenditure and body fat in humans.
584 Diabetes Metab. J. *37*, 22–29.

585 Santoro, A., McGraw, T.E., and Kahn, B.B. (2021). Insulin action in adipocytes, adipose remodeling,
586 and systemic effects. Cell Metab. *33*, 748–757.

587 Sapolsky, R.M. (2004). Why zebras don't get ulcers (New York: Holt Paperbacks).

588 Sapolsky, R.M., Krey, L.C., and McEwen, B.S. (1986). The Neuroendocrinology of Stress and Aging:
589 The Glucorticoid Cascade Hypothesis. Endocr. Rev. *7*, 284–301.

590 Sapolsky, R.M., Krey, L.C., and McEwen, B.S. (1987). The adrenocortical axis in the aged rat:
591 impaired sensitivity to both fast and delayed feedback inhibition. Neurobiol. Aging *7*, 331–335.

592 Shen, Y., Roh, H.C., Kumari, M., and Rosen, E.D. (2017). Adipocyte glucocorticoid receptor is
593 important in lipolysis and insulin resistance due to exogenous steroids, but not insulin resistance
594 caused by high fat feeding. Mol. Metab. *6*, 1150–1160.

595 Song, Z., Xiaoli, A.M., and Yang, F. (2018). Regulation and metabolic significance of De Novo
596 lipogenesis in adipose tissues. Nutrients *10*, 1–22.

597 Spiga, F., Walker, J.J., Terry, J.R., and Lightman, S.L. (2014). HPA axis-rhythms. Compr. Physiol. *4*,
598 1273–1298.

599 Strack, A.M., Bradbury, M.J., and Dallman, M.F. (1995). Corticosterone decreases nonshivering
600 thermogenesis and increases lipid storage in brown adipose tissue. Am. J. Physiol. - Regul. Integr.
601 Comp. Physiol. *268*, R183–R191.

602 Strawford, A., Antelo, F., Christiansen, M., and Hellerstein, M.K. (2004). Adipose tissue triglyceride

turnover, de novo lipogenesis, and cell proliferation in humans measured with 2H2O. Am. J. Physiol. - Endocrinol. Metab. *286*, 577–588.

VanDenBeukel, J.C., Grefhorst, A., Quarta, C., Steenbergen, J., Mastroberardino, P.G., Lombés, M., Delhanty, P.J., Mazza, R., Pagotto, U., Van Der Lely, A.J., et al. (2014). Direct activating effects of adrenocorticotropic hormone (ACTH) on brown adipose tissue are attenuated by corticosterone. FASEB J. *28*, 4857–4867.

Viengchareun, S., Penfornis, P., Zennaro, M.C., and Lombès, M. (2001). Mineralocorticoid and glucocorticoid receptors inhibit UCP expression and function in brown adipocytes. Am. J. Physiol. - Endocrinol. Metab. *280*, 640–649.

Walter, W., Sánchez-Cabo, F., and Ricote, M. (2015). GOplot: An R package for visually combining expression data with functional analysis. Bioinformatics.

Weitzman, E.D., Fukushima, D., Nogeire, C., Roffwarg, H., Gallagher, T.F., and Hellman, L. (1971). Twenty-four hour pattern of the episodic secretion of cortisol in normal subjects. J. Clin. Endocrinol. Metab. *33*, 14–22.

Yu, C.Y., Mayba, O., Lee, J. V., Tran, J., Harris, C., Speed, T.P., and Wang, J.C. (2010). Genome-wide analysis of glucocorticoid receptor binding regions in adipocytes reveal gene network involved in triglyceride homeostasis. PLoS One *5*.

Yu, G., Wang, L.G., Han, Y., and He, Q.Y. (2012). ClusterProfiler: An R package for comparing biological themes among gene clusters. Omi. A J. Integr. Biol.

AUTHOR CONTRIBUTIONS

S.T. and M.N.T. conceived the project. S.T. performed and analyzed all experiments with assistance of A.R., E.B.M., and W.Y. K.M.K. analyzed transcriptomic data. F.B.K. designed experiments and contributed to the discussion. S.T. and M.N.T wrote the paper with input from all authors.

ACKNOWLEDGEMENTS

This work was supported by National Institutes of Health RO1-DK101743, RO1-DK106241, P50-GM107615, and Stanford BioX Seed Grant funding (to M.N.T.), and the U.S. Department of Veterans Affairs I01BX000398 (FBK). Furthermore, we acknowledge the funding from the Deutsche Forschungsgemeinschaft (DFG) TH 2156/1-1 (to S.T.), the Stanford Bio-X Program and Novo Nordisk Foundation NNF16OC0018642 (to A.R.), and American Heart Association Postdoctoral Fellowship 18POST34030448 (to E.B.M.). We thank Tim McGraw, Fred Maxfield, Laura Alonso, Tobias Meyer (Weill Cornell Medicine) and the members of the Teruel Lab for discussions and critical reading of the manuscript. We also thank the Stanford Animal Histology Services (AHS) for paraffin embedding of fat tissue and performing H&E staining.

Declaration of interest

The authors declare no competing interests.

644 **FIGURE LEGENDS**
645
646 **Figure 1. Flattening of circadian glucocorticoid oscillations causes rapid adipocyte**
647 **hypertrophy.**
648 **(A)** Schematic of approach used to determine how flattening of glucocorticoid oscillations affects
649 adipocyte hypertrophy over time. The normal circadian GC oscillation pattern is shown in grey. The
650 flattened glucocorticoid pattern is shown in orange.
651 **(B)** Time course of average corticosterone levels in mice implanted with corticosterone pellets (cort-
652 pellet mice) compared to mice implanted with sham pellets (sham-pellet mice) 7 days after pellet
653 implantation. n = 8 for sham pellet; n = 8 for corticosterone pellet, mean ± SEM.
654 **(C)** Time course showing body weight gain of cort-pellet compared to sham-pellet mice. n = 11,
655 mean ± SEM. Unpaired t test (sham pellet versus cort pellet), *p < 0.05, **p < 0.01, ***p < 0.001,
656 ****p < 0.0001.
657 **(D)** Average daily food intake of each mouse per cage (n = 8). Up to 5 mice were housed in each
658 cage. Food intake was monitored for 21 days, mean ± SD. Unpaired t-test, ns = not significant.
659 **(E-G)** sWAT, vWAT, and BAT fat pad images, fat pad weight, and hematoxylin and eosin (H & E)
660 staining analysis. Fat pad images were taken 21 days after pellet implantation. Fat pad weight was
661 measured at 3, 7, 14, and 21 days after pellet implantation, n = 5-9, mean ± SD. Unpaired t test, **p <
662 0.01, ****p < 0.0001. One representative H & E staining is shown for each timepoint (n = 3). Scale
663 bars 50 μm. See also Table S1.
664
665 **Figure 2. Increasing the peak amplitude of corticosterone in the evening phase does not affect**
666 **body weight gain or lipid accumulation in WAT.**
667 **(A)** Schematic of approach used to determine how flattening of glucocorticoid oscillations affects
668 adipocyte hypertrophy over time The perturbation from the normal glucocorticoid oscillation pattern is
669 shown in orange.
670 **(B)** Time course of average corticosterone levels in mice injected with corticosterone compared to
671 mice injected with solvent control (phosphate buffer) 7 days after start of injections. n = 3-4, mean ±
672 SEM.
673 **(C)** Time course showing body weight gain of mice injected with corticosterone compared to mice
674 injected with solvent control (phosphate buffer). n = 9 for sham injection; n = 9 for corticosterone
675 injection, mean ± SEM.
676 **(D)** Average daily food intake of each mouse per cage (n = 7). Up to 5 mice were housed in each cage.
677 Food intake was monitored for 21 days, mean ± SD. Unpaired t test, **p < 0.01, ns = not significant.
678 **(E-G)** sWAT**,** vWAT, and BAT fat pad weight measured at 3, 7, 14, and 21 days after start of daily
679 injections, n = 3-8, mean ± SD. See also Table S1 and Figure S1.
680
681 **Figure 3. Flattening of glucocorticoid oscillations does not result in fat deposition in the liver,**
682 **elevated circulating triglycerides in blood serum, or defects in thermogenesis.**
683 **(A)** H&E staining of livers 21 days after sham or corticosterone pellet implantation. One representative
684 staining is shown (n = 4). Weight of livers at different time points after pellet implantation, n = 4-5,
685 mean ± SD. See also Table S1.
686 **(B)** Time courses of changes in FFA, glycerol, and triglycerides measured in blood serum over 14
687 days. n = 4-5 for pellet-implanted mice, mean ± SEM, unpaired t test, *p < 0.05, ns = not significant.
688 **(C-D)** Same as in **(A-B)** but instead for daily Sham or corticosterone injected mice, n = 3-4.
689 **(E)** Flattening of daily corticosterone oscillations in mice results in downregulation of genes involved
690 in thermogenesis. mRNA expression for UCP-1 and PGC1a measured by qPCR in BAT of pellet
691 implanted mice. Gene expression data was normalized to the expression of Tbp and is presented as
692 mean ± SEM (n = 3-4). Unpaired t test, *p < 0.05, **p < 0.01, ***p < 0.001, ns = not significant. Control
693 group are mice at start of experiment (day 0).
694 **(F)** Western Blot analysis of UCP-1 in BAT lysates.

(G) Acute cold exposure experiment of sham and cort pellet-implanted mice 21 days after pellet implantation. Mean +/- SEM; n = 8.

Figure 4. Flattening of glucocorticoid oscillations results in gene expression alterations in vWAT of genes involved in lipogenesis.
(A) Principal component analysis of vWAT from corticosterone versus sham pellet-implanted mice obtained at 3, 7, and 14 days after pellet implantation.
(B) Principal component analysis of vWAT from corticosterone and sham injected mice obtained at 3, 7, and 14 days after the start of injections.
(C) Schematic of gene expression changes in triglyceride synthesis pathways in vWAT from corticosterone versus sham pellet-implanted mice. Upregulated, unchanged, and downregulated genes are marked in red, black, and blue, respectively. Bold type mark genes with a more than 2-fold change in gene expression.
(D) Barplots showing fold-change of significantly changed vWAT genes in corticosterone versus sham pellet-implanted mice. See also Figures S4-S5 and Tables S2-S7.

Figure 5. Flattening of glucocorticoid oscillations causes hyperinsulinemia within 3 days.
(A) Time course of insulin levels in blood plasma in sham and corticosterone pellet-implanted mice (not fasted); mean +/- SEM; n = 6; unpaired t test, *$p < 0.05$, **$p < 0.01$, ****$p < 0.0001$.
(B) Blood glucose levels in sham and corticosterone pellet-implanted mice (not fasted) 14 days after pellet implantation; mean +/- SEM; n = 9; unpaired t test, **$p < 0.01$.
(C) Glucose tolerance test (GTT) of sham and corticosterone pellet-implanted mice after 21 days of treatment; mean ± SEM; n = 5; unpaired t test, *$p < 0.05$, ***$p < 0.001$, ****$p < 0.0001$.
(D) Insulin tolerance test (ITT) of sham and corticosterone pellet-implanted mice after 17 days of treatment; mean ± SEM; n = 5 for sham pellet; n = 6 for corticosterone pellet; unpaired t test, *$p < 0.05$, **$p < 0.01$.
(E) Glucose tolerance test (GTT) of sham and corticosterone injected mice after 21 days of treatment; mean ± SEM; n = 6.
(F) Insulin tolerance test (ITT) of sham and corticosterone injected mice after 17 days of treatment; mean ± SEM; n = 5 for sham injection; n = 6 for corticosterone injection.

Figure 6. The hyperinsulinemia and much of the adipocyte hypertropy are reversible when the glucocorticoid flattening stimulus is removed.
(A) Time course of insulin levels in blood plasma in sham and corticosterone pellet-implanted mice (not fasted); mean +/- SEM; n = 6; unpaired t test, *$p < 0.05$, **$p < 0.01$.
(B) Fat pad weight was measured at 21 and 42 days after pellet implantation, n = 5-9, mean ± SD. Unpaired t test, **$p < 0.01$, ****$p < 0.0001$. Data from 21 days is the same as in Figures 1E-1F, second panel.
(C) Schematic representation of the commonly discussed acute and chronic stress states, as well as a reversible intermediate state arising from three weeks of glucocorticoid flattening. Mice can mostly recover from this intermediate alert state without long-term adipocyte dysfunction.

Figure 7. Cd36ko partially protects against adipocyte hypertrophy resultng from flattening of glucocorticoid oscillations.
(A) qPCR of vWAT and BAT 3 and 14 days after cort or sham pellet implantation. Data is normalized to the expression of Tbp and is presented as mean ± SEM (n = 3-4). Unpaired t test, *$p < 0.05$, **$p < 0.01$, ***$p < 0.001$, ns = not significant. Control group are mice at start of experiment (day 0).
(B) Weight of vWAT, BAT, and sWAT fat depots 21 days after pellet implantation, n = 5-12, mean ± SD. Unpaired t test, *$p < 0.05$, ****$p < 0.0001$. See also Table S1.

745 **(C)** H&E staining of vWAT, BAT, and sWAT 21 days after pellet implantation. One representative
746 staining is shown (n = 3-5). Scale bars 50μm. See also Figure S6.
747 **(D)** Insulin levels in blood plasma in corticosterone and sham pellet-implanted Cd36ko and wild-type
748 mice (not fasted) 14 days after pellet implantation; mean +/- SEM; n = 5-7; unpaired t test, *$p < 0.05$,
749 **$p < 0.01$.
750 **(E)** Blood glucose levels in corticosterone and sham pellet-implanted Cd36ko and wild-type mice
751 (not fasted) 14 days after pellet implantation; mean +/- SEM; n = 6-9; unpaired t test, **$p < 0.01$.
752 **(F)** Scheme of how an initially protective adipocyte hypertrophy mechanism can be activated in
753 response to flattening of circadian glucocorticoid oscillations. Glucocorticoid flattening results in a
754 unique metabolic signature with high insulin, slightly lower-than-normal glucose, and normal FFA
755 levels in the circulation.
756
757

SUPPLEMENTARY FIGURES

Figure S1. Images of tissue and adipocyte sections in WAT and BAT induced by daily corticosterone injection versus sham injection.
(A-C) Lack of a visible change in size of WAT and BAT tissue and size of adipocytes in Cort injected versus Sham injected mice (n=3 mice per treatment, 25 images per mouse (20x)).

Figure S2. Flattening of corticosterone oscillations does not result in significant gene expression alterations of genes involved in lipid metabolism in liver.
(A-J) Gene expression of different genes measured by qPCR in liver after flattening corticosterone levels for 14 days. Gene expression data was normalized to the expression of Tbp and is presented as mean ± SEM (n = 3-4). Unpaired t test, $*p < 0.05$, $**p < 0.01$, ns = not significant. Control group are mice at beginning of experiment (day 0).

Figure S3. Comparison of BAT and vWAT RNAseq datasets.
(A-B) Number of significantly changed transcripts in BAT and vWAT in different comparisons of treatment methods.
(C) Number of overlapping transcripts in vWAT and BAT. See also Tables S2-S7.

Figure S4. Analysis of BAT RNAseq dataset.
(A) Principal component analysis of BAT from corticosterone versus sham pellet-implanted mice obtained at 3, 7, and 14 days after pellet implantation.
(B) Principal component analysis of BAT from corticosterone and sham injected mice obtained at 3, 7, and 14 days after the start of injections.
(C) Schematic of gene expression changes in triglyceride synthesis pathways in BAT from corticosterone versus sham pellet-implanted mice. Upregulated, unchanged, and downregulated genes are marked in red, black, and blue, respectively. Bold type mark genes with a more than 2-fold change in gene expression. See also Tables S2-S7.
(D) Barplots showing fold-change of significantly changed BAT genes in corticosterone versus sham pellet-implanted mice. See also Tables S2-S7.

Figure S5. Corticosterone measurements in mice implanted with corticosterone or sham pellets at Day 42 after pellet implantation.
(A) Blood serum corticosterone levels at Day 42 for 8 corticosterone pellet-implanted mice.
(B) Blood serum corticosterone levels at Day 42 for 8 sham pellet-implanted mice.

Figure S6. Quantification of lipid droplet size in WT and CD36KO mice implanted with corticosterone or sham pellets for 21 days.
(A-C) Frequency distributions of mean lipid droplet area in sWAT, vWAT, and BAT as analyzed using Adiposoft (mean + SEM; n=3 mice per treatment, 25 images per mouse (20x)).

801 **SUPPLEMENTARY TABLES**
802
803 **Table S1. Summary of mouse experiments.** All data was acquired after a treatment period of 21
804 days, except data for blood glucose (not fasted), FFA, glycerol, and triglyceride levels, which were
805 determined 14 days after beginning of treatment. Values are presented as mean +/- SEM; n.d. = no
806 data.
807
808 **Table S2. Gene otology (GO term) analysis of differentially expressed genes in vWAT of**
809 **corticosterone versus sham pellet-implanted mice.**
810
811 **Table S3. Gene otology (GO term) analysis of differentially expressed genes in BAT of**
812 **corticosterone versus sham pellet-implanted mice.**
813
814 **Table S4. Transcript levels of differentially expressed genes in vWAT of corticosterone versus**
815 **sham pellet-implanted mice.**
816
817 **Table S5. Gene expression levels of differentially expressed genes in vWAT of corticosterone**
818 **versus sham pellet-implanted mice.**
819
820 **Table S6. Transcript levels of differentially expressed genes in BAT of corticosterone versus**
821 **sham pellet-implanted mice.**
822
823 **Table S7. Gene expression levels of differentially expressed genes in BAT of corticosterone**
824 **versus sham pellet-implanted mice.**
825
826
827

828 **METHODS**
829

830 **Mice**

831 Mice were housed in small groups of five or fewer on a 12h light/dark cycle (lights on at 7:00 hours)
832 with food and water access ad libitum in the animal facility at Stanford University. All mice were
833 maintained on a normal chow diet and only male mice were used for experiments. All animal care and
834 experimentation was conducted in accordance with current NIH and Stanford University Institutional
835 Animal Care and Use Committee guidelines. Seven-week-old C57BL/6J male mice were purchased
836 from Jackson Laboratory (cat. 000664) and housed in the animal facility for 7 days prior the start of
837 experiments. Cd36ko mice were published before(Febbraio et al., 1999). Cd36ko breeding pairs were
838 purchased from Jackson Laboratory (cat. 019006). For the experiments, 8-week old male mice were
839 used. All mice were dissected between 13:00 and 18:00 alternating corticosterone-treated and control
840 mice. A summary of all parameters measured in mice upon different treatments can be found in
841 Extended Data, Table 1.

842 During the acute cold exposure experiments, mice were placed in individual cages with
843 minimal bedding in order to prevent nesting or huddling behavior which would interfere with adaptive
844 thermogenesis. The cages were placed in a 4 °C deli fridge for the 6-hour timecourse experiment. Core
845 body temperatures of the mice were assessed with a rectal probe thermometer (Type J/K/T
846 Thermocouple meter, Digisense, Kentscientific, USA; with rectal probe for mice RET-3, Physitemp
847 Instruments, USA) before and at one-hour intervals during the 6-hour cold exposure. Timepoint 0 was
848 taken 1 minute before the mice went into the cold.

849

850 **Corticosterone administration in mice**

851 To flatten diurnal glucocorticoid oscillations, mice were implanted subcutaneously with corticosterone
852 releasing pellets (5mg, 21-day release; Innovative Research of America, Sarasota, FL, USA, Catalog
853 number G-111). Sham pellets (Catalog number C-111) were implanted as control. For pellet

854 implantation mice were anesthetized via inhalation of isoflurane, when anesthetized an incision equal
855 in diameter to that of the pellet was made on the lateral side of the neck and the pellet inserted using
856 a trochar. Mice weighed an average of 24.1 ± 1.2 g, which results in a daily dose of 9 mg/kg/day.
857 For injections, corticosterone complexed with 2-hydroxypropyl-β-cyclodextrin (C174, Sigma)
858 was dissolved in phosphate buffer (PBS) and injected subcutaneously once daily at 17:00 for up to 21
859 days with the same corticosterone dose (9 mg/kg/day) as released by the corticosterone pellets per
860 day. PBS was injected as control.
861
862 **Measurement of corticosterone in blood serum**
863 Blood was taken at multiple time points over a 15 h time period. At the first time point, blood was taken
864 by nicking the tail vain. Blood samples collected on following time points were taken by removal of the
865 crust formed after first blood withdrawal. The blood was allowed to clot by leaving it undisturbed at
866 room temperature for 45 minutes. The clot was removed by centrifuging at 2000 x g for 15 minutes.
867 The corticosterone concentration in blood serum was determined using the Enzyme Immunoassay kit
868 (K014-H1, Arbor Assays, Michigan, USA) following the manufacturer's instructions.
869
870 **Glucose Tolerance Test**
871 Before the procedure mice were fasted for 16h in clean cages with no food or feces in the bedding. At
872 9am blood glucose levels were measured with a glucometer (Diathrive, South Salt Lake, Utah, USA)
873 by obtaining a drop of blood from the tail. Subsequently, mice received 2 g of glucose (Sigma G8270)
874 / kg of body weight by intraperitoneal injection. Blood glucose levels were measured again after 15,
875 30, 60, and 120 min after injection.
876 To measure insulin levels 20 μl of blood were collected from the tail before glucose injection
877 and on every following time point and mixed with heparin. The blood plasma was prepared by
878 centrifugation at 2000 x g for 15 minutes. The insulin concentration in blood plasma was determined

879 using the Ultra Sensitive Mouse Insulin ELISA Kit (Cat. 90080, Crystal Chem, Illinois, USA) following
880 the manufacturer's instructions.
881
882 **Insulin Tolerance Test**
883 Before the procedure mice were fasted for 6h in clean cages with no food or feces in the bedding
884 starting at 9am. Blood glucose levels were measured with a glucometer (Diathrive, South Salt Lake,
885 Utah, USA) by obtaining a drop of blood from the tail. Subsequently, mice were injected with 0.75
886 units/kg body weight of human insulin (Sigma I9278) by intraperitoneal injection. Blood glucose levels
887 were measured again after 15, 30, 45, 60, and 120 min after injection.
888 To measure insulin levels 20 μl of blood were collected from the tail before glucose injection and on
889 every following time point and mixed with heparin. The blood plasma was prepared by centrifugation
890 at 2000 x g for 15 minutes. The insulin concentration in blood plasma was determined using the Ultra
891 Sensitive Mouse Insulin ELISA Kit (Cat. 90080, Crystal Chem, Illinois, USA) following the
892 manufacturer's instructions.
893
894 **Measuring concentrations of FFA, glycerol, and triglycerides**
895 FFA contents in blood serum were determined the Free Fatty Acid Quantitation Kit (Sigma, MAK044)
896 following the manufacturers' protocols. Glycerol and triglyceride concentrations in blood serum were
897 measured using the Triglyceride Determination Kit (Sigma, TR0100) following the manufacturer's
898 instructions.
899
900 **Histology**
901 For histological examination interscapular brown adipose tissue (BAT), inguinal white adipose tissue
902 (sWAT), and epididymal white adipose tissue (vWAT) were fixed in 4% formalin for 24h directly after
903 dissection. Tissues were rinsed and stored in 95% until embedding in paraffin. Paraffin blocks were
904 sectioned (10μm) and sections mounted on glass slides and stained with hematoxylin and eosin (H &

905 E). Images were taken at 20x magnification and the adipocyte area was calculated using the Fiji
906 software plug-in Adiposoft (Galarraga et al., 2012).
907
908 **Reverse transcription quantitative polymerase chain reaction**
909 Total RNA was extracted from fat tissues using the RNeasy Lipid Tissue Mini Kit (Qiagen, Hilden,
910 Germany) and from liver using the RNeasy Mini Kit (Qiagen, Hilden, Germany). Equal amounts of
911 RNA were reverse transcribed to cDNA using the iScript cDNA Synthesis system (Bio-Rad, Hercules,
912 CA, USA). Relative transcript amounts were measured by qPCR using PowerUp SYBR Green Master
913 Mix (Appliedbiosystems, Vilnius, Lithuania). All expression data were normalized to TATA-binding
914 protein (Tbp) expression. The primer sequences were as follows: Cd36 forward → 5'-ATG GGC TGT
915 GAT CGG AAC TG-3'; Cd36 reverse → 5'-TTT GCC ACG TCA TCT GGG TTT-3'; Tbp forward → 5'-
916 GAA GCT GCG GTA CAA TTC CAG-3'; Tbp reverse → 5'-CCC CTT GTA CCC TTC ACC AAT-3';
917 Ucp1 forward → 5'-AGC CGG CTT AAT GAC TGG AG-3'; Ucp1 reverse → 5'-TCT GTA GGC TGC
918 CCA ATG AAC-3'; Angptl4 forward → 5'- CAT CCT GGG ACG AGA TGA ACT -3'; Angptl4 reverse →
919 5'- TGA CAA GCG TTA CCA CAG GC -3'; Pepck forward → 5'- CTG CAT AAC GGT CTG GAC TTC
920 -3'; Pepck reverse → 5'- GCC TTC CAC GAA CTT CCT CAC -3'; Lipe (Hsl) forward → 5'- GAT TTA
921 CGC ACG ATG ACA CAG T -3'; Lipe (Hsl) reverse → 5'- ACC TGC AAA GAC ATT AGA CAG C -3';
922 Glut4 forward → 5'- ATC ATC CGG AAC CTG GAG G -3'; Glut4 reverse → 5'- CGG TCA GGC GCT
923 TTA GAC TC -3'; Srebp1 forward → 5'- TGA CCC GGC TAT TCC GTG A -3'; Srebp1 reverse → 5'-
924 CTG GGC TGA GCA ATA CAG TTC -3'; Fasn forward → 5'- GGA GGT GGT GAT AGC CGG TAT -
925 3'; Fasn reverse → 5'- TGG GTA ATC CAT AGA GCC CAG -3'; Hsd11ß1 forward → 5'- GGA GCC
926 CAT GTG GTA TTG ACT -3'; Hsd11ß1 reverse → 5'- CCG CAA ATG TCA TGT CTT CCA T -3'; Dgat2
927 forward → 5'- GCG CTA CTT CCG AGA CTA CTT -3'; Dgat2 reverse → 5'- GGG CCT TAT GCC
928 AGG AAA CT -3'; Atgl (Pnpla2) forward → 5'- ATG TTC CCG AGG GAG ACC AA -3'; Atgl (Pnpla2)
929 reverse → 5'- GAG GCT CCG TAG ATG TGA GTG -3'.
930

931 **RNAseq**

932 RNA was extracted from BAT or vWAT using the RNeasy Lipid Tissue Mini Kit (Qiagen, Hilden,
933 Germany). For each condition (sham pellet, corticosterone pellet, sham injection, corticosterone
934 injection) RNA was extracted from 4 mice per time point (3, 7, 14 days). RNA was also isolated from
935 4 mice before start of treatment (day 0). RNA quality of all samples was evaluated by Bioanalyzer
936 2100 High Sensitivity RNA Analysis chips (Agilent, Cat. 5067-1513) which displayed intact RNA
937 integrity. mRNA samples were concentrated to ≤ 5 μl by MinElute column (QIAGEN, Cat. 74204). For
938 generation of RNA-seq libraries, polyadenylated mRNA was isolated from 300 ng of total RNA by
939 incubation with oligo-DT attached magnetic beads and followed by strand-specific library preparation
940 using the TruSeq Stranded mRNA Library Preparation kit (Ilumina, Cat. 20020595). Briefly, isolated
941 polyadenylated mRNA was fragmented using divalent cations under elevated temperature and 1st and
942 2nd strands DNA were synthesized using SuperScript II Reverse Transcriptase (provided with Ilumina
943 kit). A-tailing and adapter ligation was performed according to the manufacturer's protocol; the
944 resulting dsDNA was enriched in a PCR reaction based on predetermined CT values and cleaned
945 using AMPure XP beads (provided with Ilumina kit). Concentrations of enriched dsDNA fragments with
946 specific adapters were determined and base pair average size and library integrity were analyzed
947 using the Bioanalyzer DNA High Sensitivity chips (Agilent, Cat. 5067-4626). Samples were pooled and
948 sequenced on the Illumina NextSeq 500/550 High Output platform (Illumina, FC-404-2002) up to 18
949 samples per lane with 1% PhiX spike as a control.

950 To assess the read quality of the raw FASTQ files we used FastQC (Andrews and Babraham
951 Bioinformatics, 2010) (v0.11.7). Pseudo-alignment of the reads to the mouse reference transcriptome
952 (Mus_musculus.GRCm38.cdna) was carried out using Kallisto (Bray et al., 2016) (v0.44.0) with the
953 quantification algorithm enabled, the number of bootstraps set to 100, and ran in paired-end mode.
954 The Kallisto output files imported to R with Sleuth, and the transcripts per million (TPM) were used for
955 downstream differential expression analysis (Pimentel et al., 2017).

956 We used the Sleuth package to identify differentially expressed genes with the full model
957 consisting of treatment, lane, replicate, and day and the reduced model consisting of lane and
958 replicate. This allowed us to identify genes that were differentially expressed based on treatment (i.e.
959 corticosterone pellet vs sham pellet) and time. All downstream analysis was done on transcripts that
960 were considered significant from the DESeq2 analysis (likelihood ratio test with a FDR less than 0.05).
961 Outlier samples were identified by both clustering and PCA analysis and removed. The number of
962 differentially expressed genes after removing outliers increased by 1,668, with all but 31 genes
963 common between the two models.
964 For more information, please see https://kylekovary.shinyapps.io/Flattened-diurnal-
965 glucocorticoid-oscillations/.
966
967 **Gene Ontology (GO) Analysis**
968 GO term analysis was done using the clusterProfiler package(Yu et al., 2012). GO terms of interest
969 were identified by calculating the adjusted p-value between two sample groups (i.e. corticosterone
970 pellet vs. sham pellet) as well as a z score for general trends of increased or decreased differential
971 expression of the genes within the GO terms. The z score is defined as the number of genes within
972 the GO term with an absolute value log2 fold change greater than or equal to 1.5 (fold change > 1.5
973 or < 0.67) divided by the square root of the total number of genes assigned to that GO term(Walter et
974 al., 2015).
975
976 **Western Blot Analysis**
977 For western blot analysis 10mg of fat tissue were lysed in 50 mM Tris-HCl, 1 % Nonidet P-40, 0.1 %
978 sodium dodecyl sulfate (SDS) and 0.15 M NaCl, pH 8, supplemented with protease inhibitors
979 (cOmplete, Mini, EDTA-free, Sigma Aldrich). For preparation of tissue lysates, a homogenizer (Fisher
980 Scientific) was used and cell debris removed by centrifugation at max speed for 20 min at 4 °C. Protein
981 concentrations were determined using the bicinchoninic acid (BCA) protein assay kit (Pierce,

982 Rockford, USA). 50 µg of proteins of tissue lysates were boiled for 5 min at 95°C in NuPAGE LDS
983 sample buffer containing 1x reducing agent (Invitrogen). Lysates were separated by SDS–PAGE using
984 the XCell SureLock Electrophoresis Cell on NuPAGE Novex 4%–12% Bis-Tris Protein Gels
985 (Invitrogen). Proteins were transferred onto polyvinylidene fluoride membranes (Thermo Scientific)
986 using the XCell II Blot Module (Invitrogen). Membranes were blocked by incubating with TBS with
987 0.1% Tween-20 containing 3% non-fat milk for 2h at room temperature or overnight at 4°C. After
988 blocking, membranes were exposed to the primary antibody (UCP-1; used 1:800) overnight at 4°C.
989 After washing (TBS with 0.1% Tween-20), the membranes were incubated for 2 h with the secondary
990 antibody. The membranes were washed (TBS with 0.1% Tween-20) and developed with the
991 Supersignal West Femto chemiluminescence substrate (Pierce, Rockford, USA). Peroxidase activity
992 was detected with a Lumi Imager device (ImageQuant LAS 4000mini, GE Healthcare). The primary
993 antibody UCP-1 was purchased from α-Diagnostics (Catalog No. UCP11-A). The secondary antibody
994 was purchased from Cell Signaling (α-rabbit: Catalog No. #7074).
995
996 **Statistics**
997 All data are represented as mean ± SD or mean ± SEM and analyzed by Students t test using
998 GraphPad Prism software. n indicates the number of animals per group or number of independent
999 experiments. Results were considered significant if $p < 0.05$.
1000
1001
1002

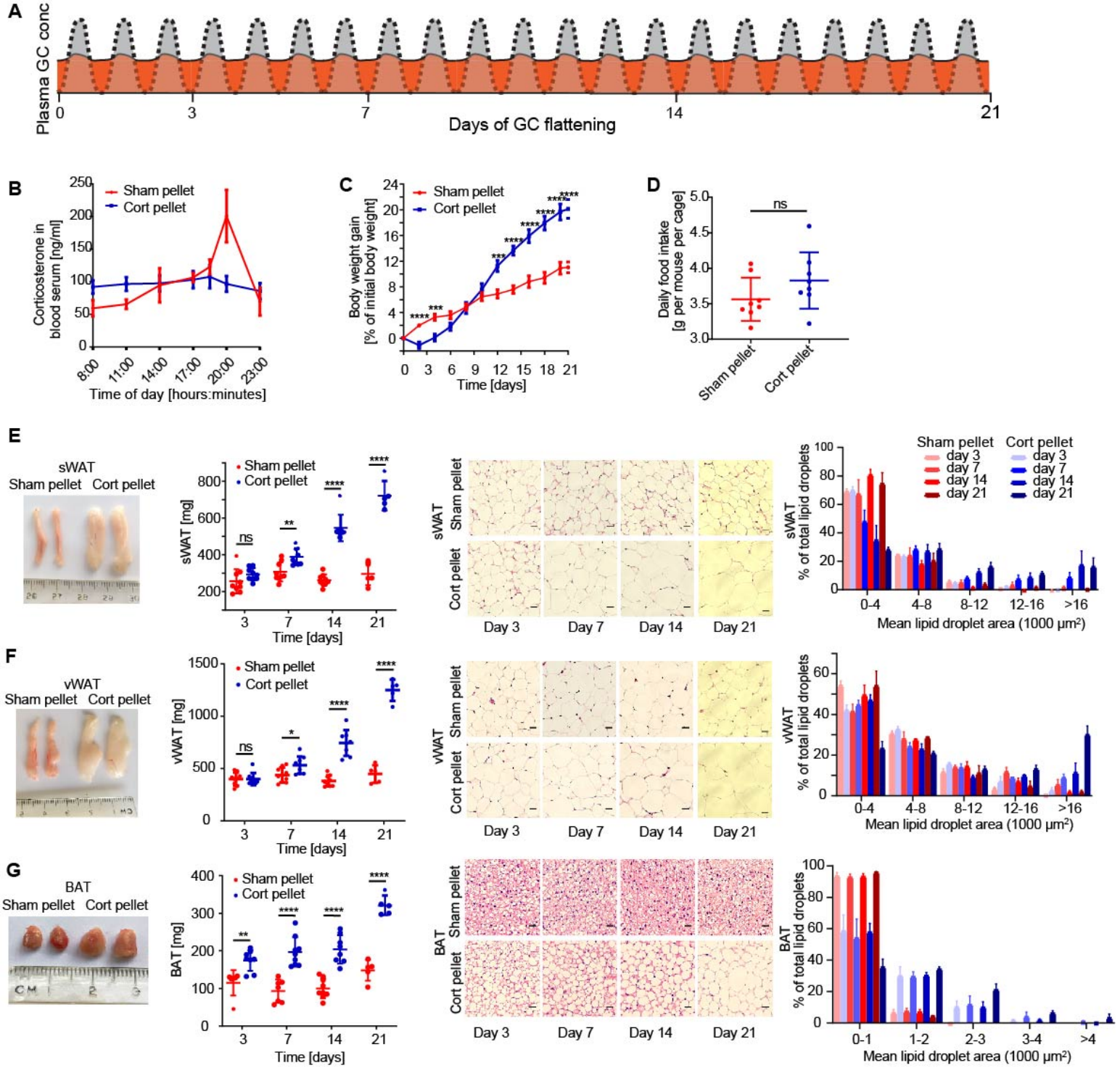

Figure 1. Flattening of circadian glucocorticoid oscillations causes rapid adipocyte hypertrophy.
(A) Schematic of approach used to determine how flattening of glucocorticoid oscillations affects adipocyte hypertrophy over time. The normal circadian GC oscillation pattern is shown in grey. The flattened glucocorticoid pattern is shown in orange.
(B) Time course of average corticosterone levels in mice implanted with corticosterone pellets (cort-pellet mice) compared to mice implanted with sham pellets (sham-pellet mice) 7 days after pellet implantation. n = 8 for sham pellet; n = 8 for corticosterone pellet, mean ± SEM.
(C) Time course showing body weight gain of cort-pellet compared to sham-pellet mice. n = 11, mean ± SEM. Unpaired t test (sham pellet versus cort pellet), *$p < 0.05$, **$p < 0.01$, ***$p < 0.001$, ****$p < 0.0001$.
(D) Average daily food intake of each mouse per cage (n = 8). Up to 5 mice were housed in each cage. Food intake was monitored for 21 days, mean ± SD. Unpaired t-test, ns = not significant.
(E-G) sWAT, vWAT, and BAT fat pad images, fat pad weight, and hematoxylin and eosin (H & E) staining analysis. Fat pad images were taken 21 days after pellet implantation. Fat pad weight was measured at 3, 7, 14, and 21 days after pellet implantation, n = 5-9, mean ± SD. Unpaired t test, **$p < 0.01$, ****$p < 0.0001$. One representative H & E staining is shown for each timepoint (n = 3). Scale bars 50 μm. See also Table S1.

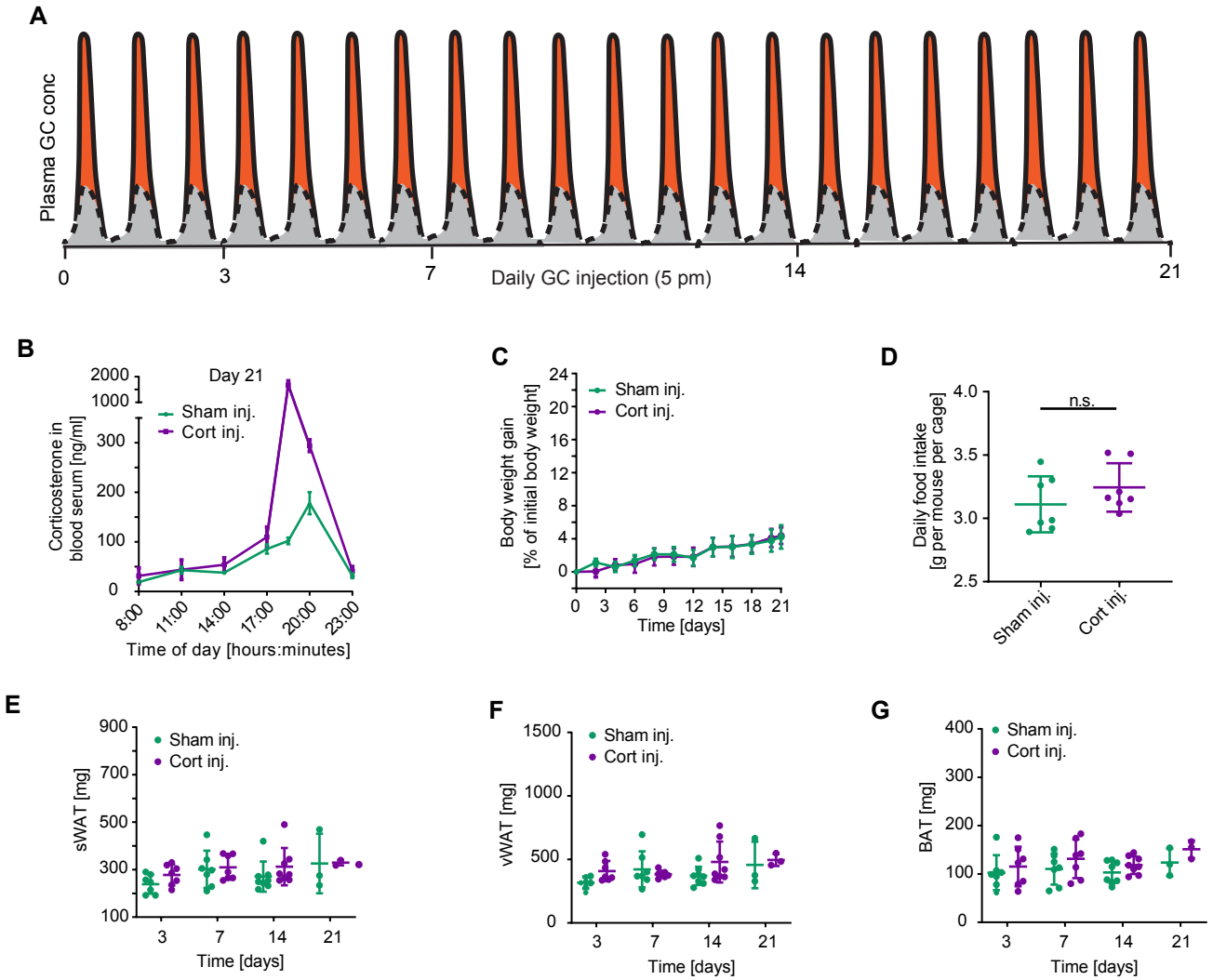

Figure 2. Increasing the peak amplitude of corticosterone in the evening phase does not affect body weight gain or lipid accumulation in WAT.

(A) Schematic of approach used to determine how flattening of glucocorticoid oscillations affects adipocyte hypertrophy over time The perturbation from the normal glucocorticoid oscillation pattern is shown in orange.

(B) Time course of average corticosterone levels in mice injected with corticosterone compared to mice injected with solvent control (phosphate buffer) 7 days after start of injections. n = 3-4, mean ± SEM.

(C) Time course showing body weight gain of mice injected with corticosterone compared to mice injected with solvent control (phosphate buffer). n = 9 for sham injection; n = 9 for corticosterone injection, mean ± SEM.

(D) Average daily food intake of each mouse per cage (n = 7). Up to 5 mice were housed in each cage. Food intake was monitored for 21 days, mean ± SD. Unpaired t test, $^{**}p < 0.01$, ns = not significant.

(E-G) sWAT, vWAT, and BAT fat pad weight measured at 3, 7, 14, and 21 days after start of daily injections, n = 3-8, mean ± SD. See also Table S1 and Figure S1.

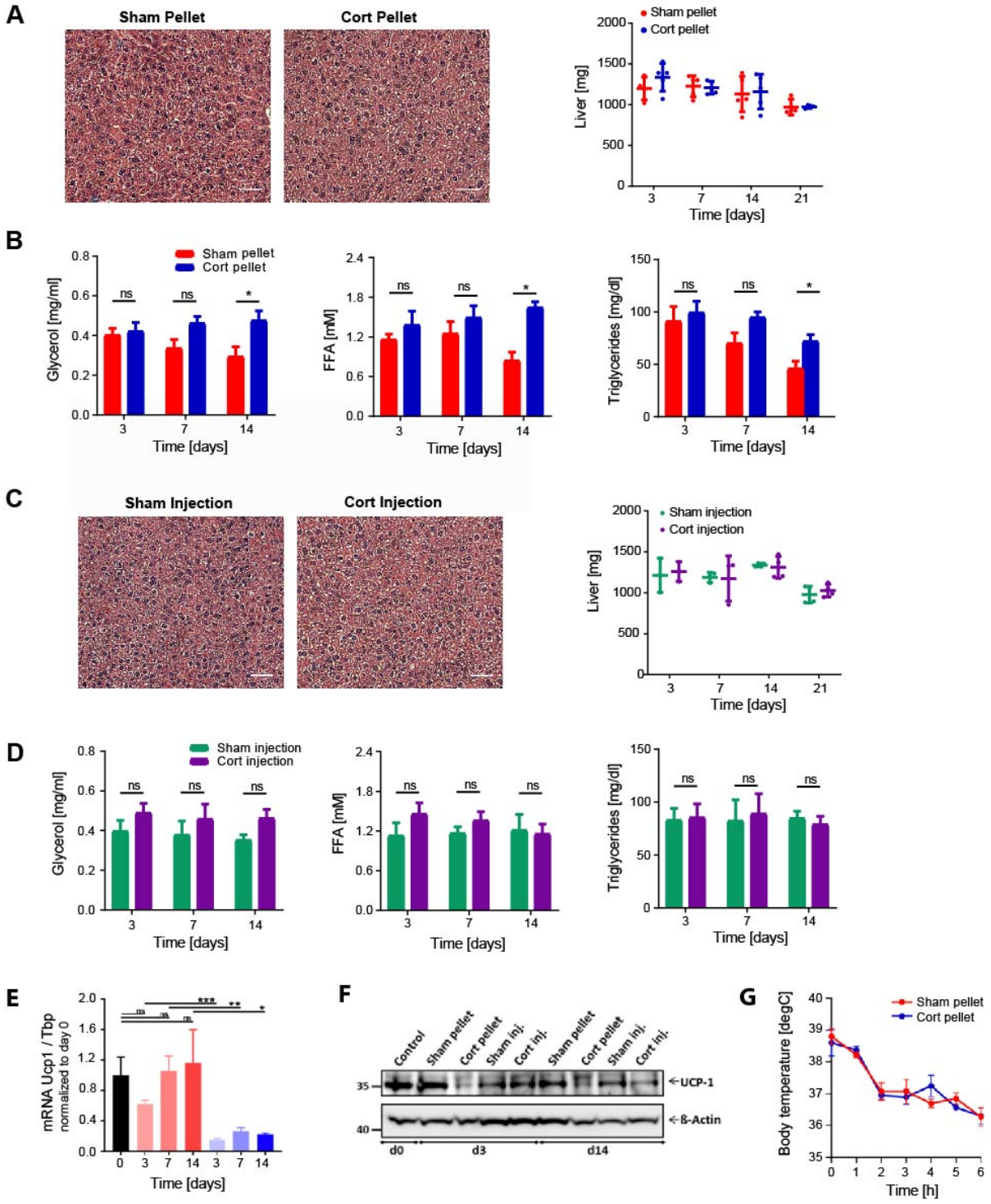

Figure 3. Flattening of glucocorticoid oscillations does not result in fat deposition in the liver, elevated circulating triglycerides in blood serum, or defects in thermogenesis.

(A) H&E staining of livers 21 days after sham or corticosterone pellet implantation. One representative staining is shown (n = 4). Weight of livers at different time points after pellet implantation, n = 4-5, mean ± SD. See also Table S1.

(B) Time courses of changes in FFA, glycerol, and triglycerides measured in blood serum over 14 days. n = 4-5 for pellet-implanted mice, mean ± SEM, unpaired t test, *$p < 0.05$, ns = not significant.

(C-D) Same as in (A-B) but instead for daily Sham or corticosterone injected mice, n = 3-4.

(E) Flattening of daily corticosterone oscillations in mice results in downregulation of genes involved in thermogenesis. mRNA expression for UCP-1 and PGC1a measured by qPCR in BAT of pellet implanted mice. Gene expression data was normalized to the expression of Tbp and is presented as mean ± SEM (n = 3-4). Unpaired t test, *$p < 0.05$, **$p < 0.01$, ***$p < 0.001$, ns = not significant. Control group are mice at start of experiment (day 0).

(F) Western Blot analysis of UCP-1 in BAT lysates.

(G) Acute cold exposure experiment of sham and cort pellet-implanted mice 21 days after pellet implantation. Mean +/- SEM; n = 8.

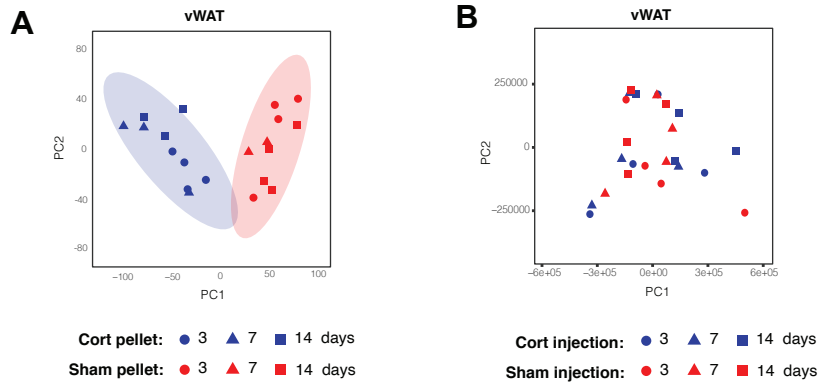

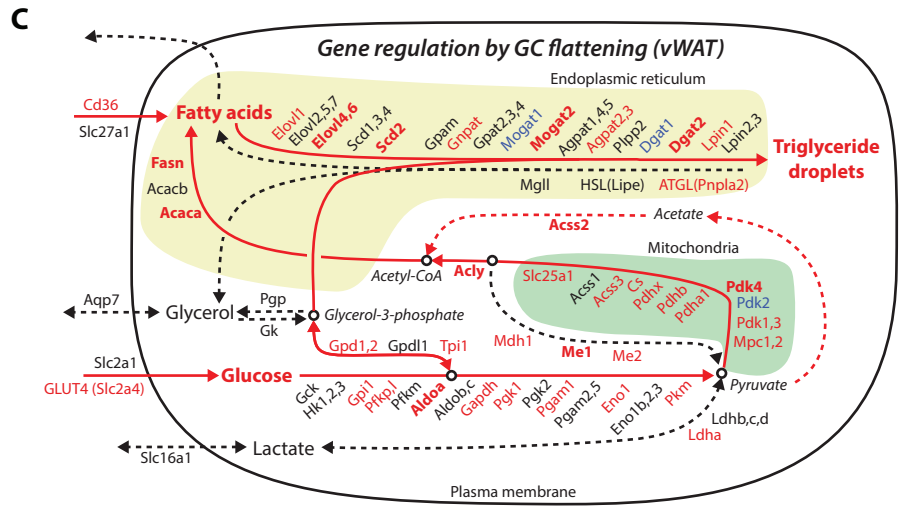

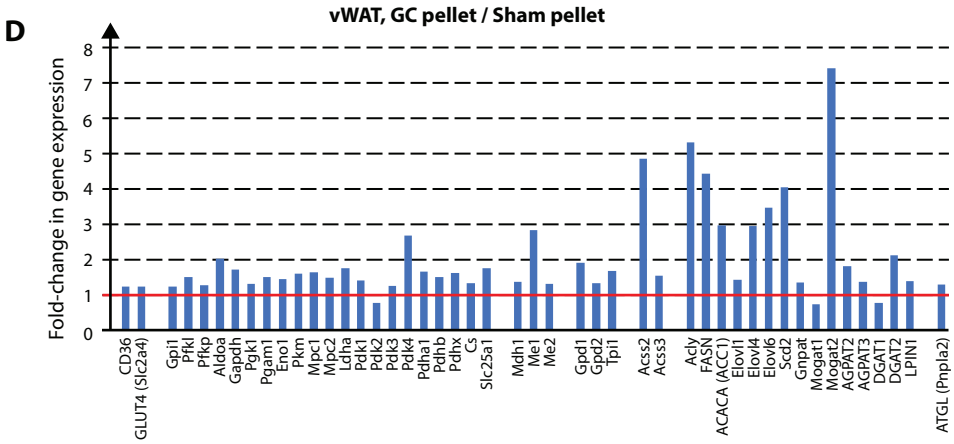

Figure 4. Flattening of glucocorticoid oscillations results in gene expression alterations in vWAT of genes involved in lipogenesis.

(A) Principal component analysis of vWAT from corticosterone versus sham pellet-implanted mice obtained at 3, 7, and 14 days after pellet implantation.

(B) Principal component analysis of vWAT from corticosterone and sham injected mice obtained at 3, 7, and 14 days after the start of injections.

(C) Schematic of gene expression changes in triglyceride synthesis pathways in vWAT from corticosterone versus sham pellet-implanted mice. Upregulated, unchanged, and downregulated genes are marked in red, black, and blue, respectively. Bold type mark genes with a more than 2-fold change in gene expression.

(D) Barplots showing fold-change of significantly changed vWAT genes in corticosterone versus sham pellet-implanted mice. See also Figures S4-S5 and Tables S2-S7.

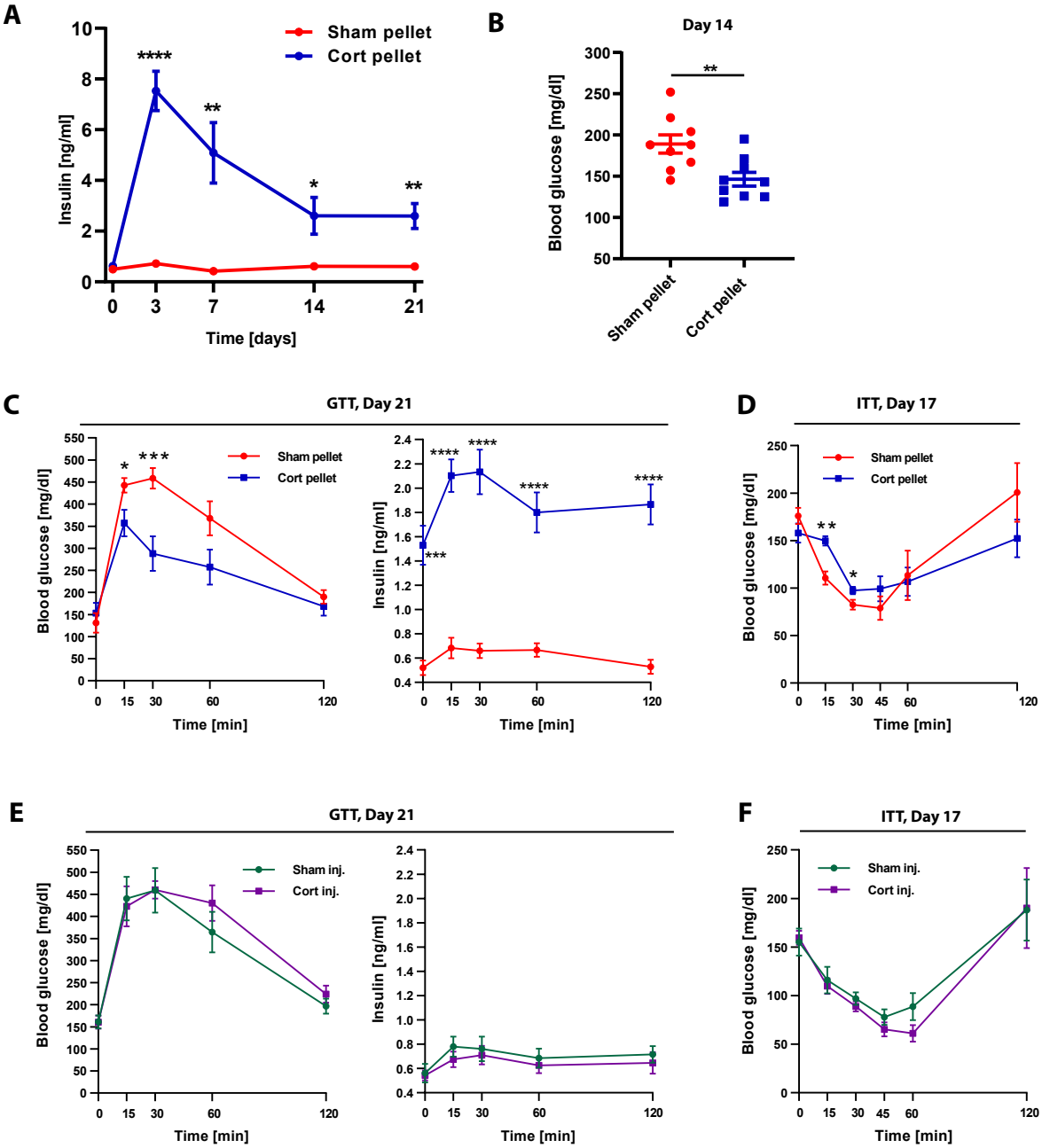

Figure 5. Flattening of glucocorticoid oscillations causes hyperinsulinemia within 3 days.
(A) Time course of insulin levels in blood plasma in sham and corticosterone pellet-implanted mice (not fasted); mean +/- SEM; n = 6; unpaired t test, *p < 0.05, **p < 0.01, ****p < 0.0001.
(B) Blood glucose levels in sham and corticosterone pellet-implanted mice (not fasted) 14 days after pellet implantation; mean +/- SEM; n = 9; unpaired t test, **p < 0.01.
(C) Glucose tolerance test (GTT) of sham and corticosterone pellet-implanted mice after 21 days of treatment; mean ± SEM; n = 5; unpaired t test, *p < 0.05, ***p < 0.001, ****p < 0.0001.
(D) Insulin tolerance test (ITT) of sham and corticosterone pellet-implanted mice after 17 days of treatment; mean ± SEM; n = 5 for sham pellet; n = 6 for corticosterone pellet; unpaired t test, *p < 0.05, **p < 0.01.
(E) Glucose tolerance test (GTT) of sham and corticosterone injected mice after 21 days of treatment; mean ± SEM; n = 6.
(F) Insulin tolerance test (ITT) of sham and corticosterone injected mice after 17 days of treatment; mean ± SEM; n = 5 for sham injection; n = 6 for corticosterone injection.

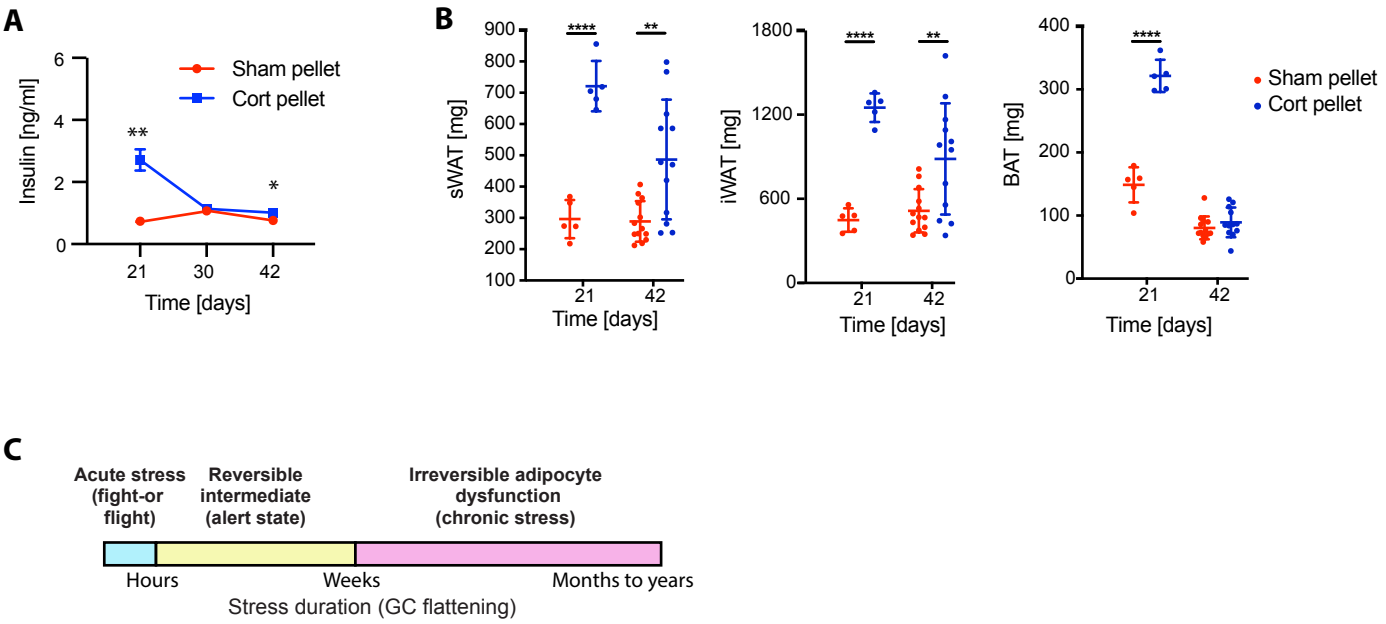

Figure 6. The hyperinsulinemia and much of the adipocyte hypertropy are reversible when the glucocorticoid flattening stimulus is removed.

(A) Time course of insulin levels in blood plasma in sham and corticosterone pellet-implanted mice (not fasted); mean +/- SEM; n = 6; unpaired t test, *p < 0.05, **p < 0.01.

(B) Fat pad weight was measured at 21 and 42 days after pellet implantation, n = 5-9, mean ± SD. Unpaired t test, **p < 0.01, ****p < 0.0001. Data from 21 days is the same as in Figures 1E-1F, second panel.

(C) Schematic representation of the commonly discussed acute and chronic stress states, as well as a reversible intermediate state arising from three weeks of glucocorticoid flattening. Mice can mostly recover from this intermediate alert state without long-term adipocyte dysfunction.

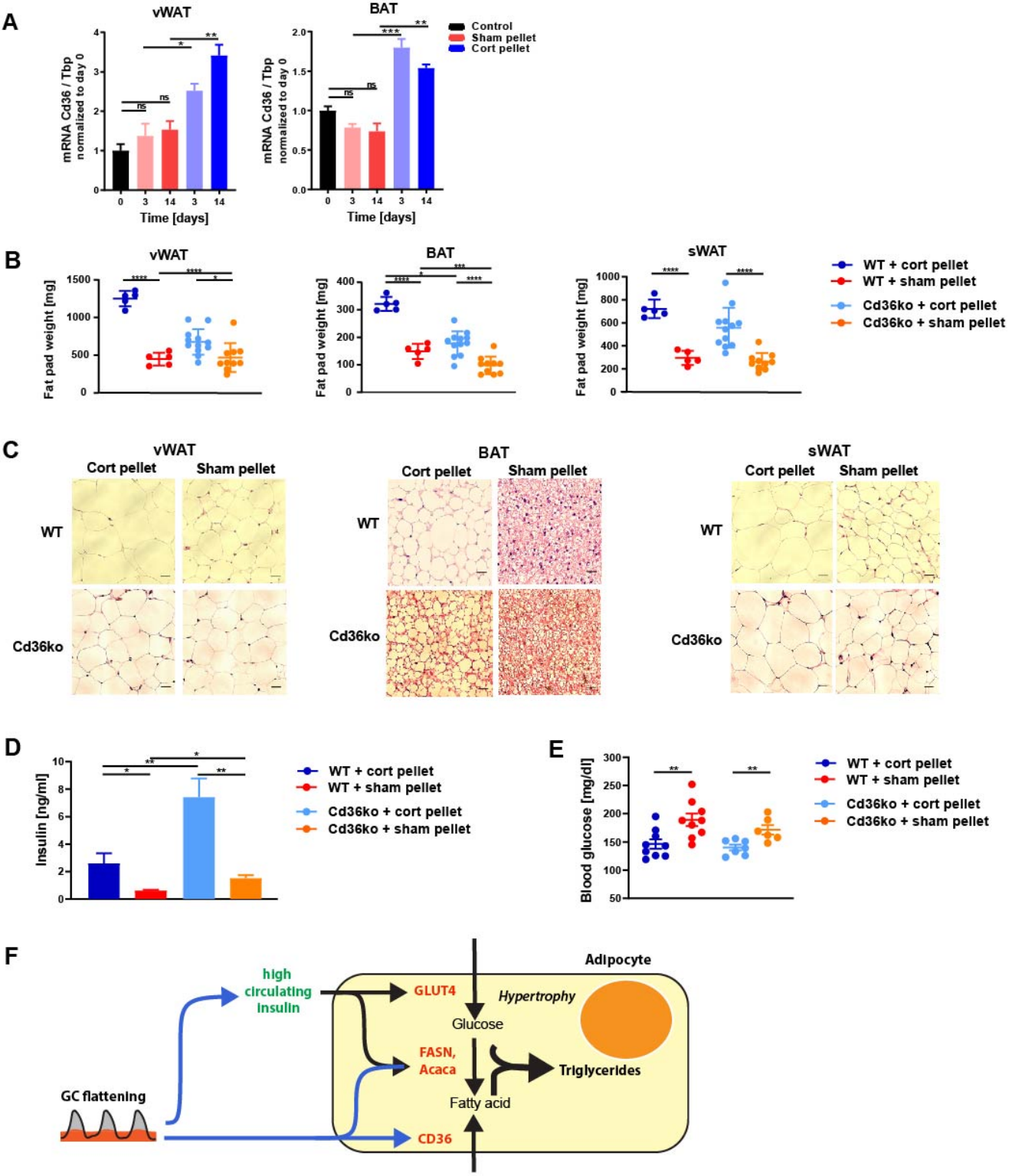

Figure 7. Cd36ko partially protects against adipocyte hypertrophy resultng from flattening of glucocorticoid oscillations.
(A) qPCR of vWAT and BAT 3 and 14 days after cort or sham pellet implantation. Data is normalized to the expression of Tbp and is presented as mean ± SEM (n = 3-4). Unpaired t test, *p < 0.05, **p < 0.01, ***p < 0.001, ns = not significant. Control group are mice at start of experiment (day 0).
(B) Weight of vWAT, BAT, and sWAT fat depots 21 days after pellet implantation, n = 5-12, mean ± SD. Unpaired t test, *p < 0.05, ****p < 0.0001. See also Table S1.
(C) H&E staining of vWAT, BAT, and sWAT 21 days after pellet implantation. One representative staining is shown (n = 3-5). Scale bars 50μm. See also Figure S6.
(D) Insulin levels in blood plasma in corticosterone and sham pellet-implanted Cd36ko and wild-type mice (not fasted) 14 days after pellet implantation; mean +/- SEM; n = 5-7; unpaired t test, *p < 0.05, **p < 0.01.
(E) Blood glucose levels in corticosterone and sham pellet-implanted Cd36ko and wild-type mice (not fasted) 14 days after pellet implantation; mean +/- SEM; n = 6-9; unpaired t test, **p < 0.01.
(F) Scheme of how an initially protective adipocyte hypertrophy mechanism can be activated in response to flattening of circadian glucocorticoid oscillations. Glucocorticoid flattening results in a unique metabolic signature with high insulin, slightly lower-than-normal glucose, and normal FFA levels in the circulation.